THE JOURNAL OF BIOLOGICAL CHEMISTRY VOL. 287, NO. 53, pp. 44301–44319, December 28, 2012

Identification of Three Residues Essential for 5-Hydroxytryptamine 2A-Metabotropic Glutamate 2 (5-HT_{2A}·mGlu2) Receptor Heteromerization and Its Psychoactive Behavioral Function*

Received for publication, August 23, 2012, and in revised form, November 1, 2012 Published, JBC Papers in Press, November 5, 2012, DOI 10.1074/jbc.M112.413161

José L. Moreno[‡], Carolina Muguruza[§1], Adrienne Umali[‡], Steven Mortillo[¶], Terrell Holloway[‡], Fuencisla Pilar-Cuéllar[‡2], Giuseppe Mocci[‡3], Jeremy Seto[‖], Luis F. Callado[§], Rachael L. Neve, Graeme Milligan[‡‡], Stuart C. Sealfon[¶‖§§¶¶], Juan F. López-Giménez[‡‡||||], J. Javier Meana[§], Deanna L. Benson[¶¶¶], and Javier González-Maeso[‡‖¶¶4]**

*From the Departments of [‡]Psychiatry, [‖]Neurology, and [¶]Neuroscience, [§§]Center for Translational Systems Biology, and [¶¶]Friedman Brain Institute, Mount Sinai School of Medicine, New York, New York 10029, the [§]Department of Pharmacology and Centro de Investigación Biomédica en Red de Salud Mental, University of the Basque Country (Universidad del País Vasco/Euskal Herriko Unibertsitatea), E-48490 Leioa, Bizkaia, Spain, the [||||]Instituto de Biomedicina y Biotecnología de Cantabria, Facultad de Medicina, E-39011 Santander, Spain, the [‡‡]Molecular Pharmacology Group, Institute of Molecular, Cell, and Systems Biology, College of Medical, Veterinary, and Life Sciences, University of Glasgow, Glasgow G12 8QQ, Scotland, United Kingdom, and the **Department of Brain and Cognitive Sciences, Massachusetts Institute of Technology, Cambridge, Massachusetts 02139*

Background: The 5-HT_{2A}·mGlu2 receptor heterocomplex is involved in psychosis.
Results: Substitution of Ala-677$^{4.40}$, Ala-681$^{4.44}$, and Ala-685$^{4.48}$ in mGlu2 abolishes the behavioral effects of hallucinogenic 5-HT_{2A} agonists.
Conclusion: Three residues at transmembrane domain 4 of mGlu2 are necessary to form the 5-HT_{2A}·mGlu2 receptor heterocomplex.
Significance: These results provide insight into the structure and behavioral function of the 5-HT_{2A}·mGlu2 receptor heterocomplex.

Serotonin and glutamate G protein-coupled receptor (GPCR) neurotransmission affects cognition and perception in humans and rodents. GPCRs are capable of forming heteromeric complexes that differentially alter cell signaling, but the role of this structural arrangement in modulating behavior remains unknown. Here, we identified three residues located at the intracellular end of transmembrane domain four that are necessary for the metabotropic glutamate 2 (mGlu2) receptor to be assembled as a GPCR heteromer with the serotonin 5-hydroxytryptamine 2A (5-HT_{2A}) receptor in the mouse frontal cortex. Substitution of these residues (Ala-677$^{4.40}$, Ala-681$^{4.44}$, and Ala-685$^{4.48}$) leads to absence of 5-HT_{2A}·mGlu2 receptor complex formation, an effect that is associated with a decrease in their heteromeric ligand binding interaction. Disruption of heteromeric expression with mGlu2 attenuates the psychosis-like effects induced in mice by hallucinogenic 5-HT_{2A} agonists. Furthermore, the ligand binding interaction between the components of the 5-HT_{2A}·mGlu2 receptor heterocomplex is up-regulated in the frontal cortex of schizophrenic subjects as compared with controls. Together, these findings provide structural evidence for the unique behavioral function of a GPCR heteromer.

G protein-coupled receptors (GPCRs)[5] represent the largest family of plasma membrane proteins and are responsible for much of the transmembrane signal transduction in living cells (1, 2). These signaling molecules have in common a central core domain that is composed of seven transmembrane (TM) α-helices, with an extracellular N terminus and an intracellular carboxyl tail (3). GPCRs have been traditionally considered to exist as monomeric structural units that couple to intracellular heterotrimeric G proteins upon ligand binding. The monomeric model of receptor signaling is supported by observations based

* This work was supported, in whole or in part, by National Institutes of Health Grants R01 MH084894 (to J. G. M.), R01 NS37731 (to D. L. B.), and P01 DA12923 (to S. C. S.). This work was also supported by Dainippon Sumitomo Pharma (to J. G. M.), National Alliance for Research on Schizophrenia and Depression (to J. G. M.), The Mortimer D. Sackler Foundation (to J. G. M.), Ministerio de Ciencia e Innovación Grant SAF2009-084609 (to J. J. M.), Basque Government Grant IT-199-07 (to J. J. M.), Consejo Superior de Investigaciones Científicas Grants PA1003176 and 200980I110 (to J. F. L.-G.), and Medical Research Council United Kingdom Grant G0900050 (to G. M.).
[1] Recipient of a predoctoral fellowship from University of the Basque Country, Spain.
[2] Recipient of a postdoctoral fellowship from Fundación Alicia Koplowitz, Spain.
[3] Recipient of a predoctoral fellowship from Consejo Superior de Investigaciones Científicas, Spain.
[4] To whom correspondence should be addressed: Dept. of Psychiatry, Mount Sinai School of Medicine, 1425 Madison Ave., Box 1229, New York, NY 10029. Tel: 212-659-8873; Fax: 212-996-9785; E-mail: Javier.Maeso@mssm.edu.

[5] The abbreviations used are: GPCR, G protein-coupled receptor; 5-HT, 5-hydroxytryptamine (serotonin); DOI, 1-(2,5-dimethoxy-4-iodophenyl)-2-aminopropane; eYFP, enhanced yellow fluorescent protein; FCM, flow cytometry; HSV, herpes simplex virus; LY379268, (1*R*,4*R*,5*S*,6*R*)-4-amino-2-oxabicyclo[3.1.0]hexane-4,6-dicarboxylic acid; mGlu, metabotropic glutamate; TM, transmembrane domain; ANOVA, analysis of variance.

on assays that measured agonist binding and G protein coupling of a single purified monomeric family A GPCR, including the β_2-adrenoreceptor (4) and rhodopsin (5), reconstituted into a phospholipid bilayer. These findings in reconstituted systems provide clear evidence that a single receptor is sufficient for fully functional G protein activation. Nevertheless, it is now well accepted that GPCRs also assemble into homomeric (6–9) and heteromeric (10, 11) structural units. Heteromers of GPCRs are of particular interest because they have been suggested to exhibit specific pharmacological and signaling properties as compared with homomeric GPCRs *in vitro* in tissue culture (12–16). The functional significance of heteromeric GPCR complexes in whole animal models remains largely unexplored.

Another point of interest is related to the structural arrangement between the components of GPCR homo- and heterooligomers. There is incontrovertible evidence about the domains that contribute to family C GPCR complex formation; these include both extracellular disulfide bonds and intracellular coiled-coil domains in the case of metabotropic glutamate (mGlu) and GABA$_B$ receptors, respectively (17, 18). Family A GPCRs, such as rhodopsin, α_{1b}-adrenergic, and dopamine D$_2$ receptors, have been shown to be assembled into homo-oligomeric complexes with symmetrical contact points involving TM4 and the extracellular end of TM1 (6, 7, 19). Much less is known about the residues located at the GPCR heteromeric interface.

Family A serotonin 5-HT$_{2A}$ and family C mGlu2 receptors have been implicated in the pathophysiology of schizophrenia and other psychotic disorders, as well as in the molecular mechanism of action of hallucinogenic drugs of abuse (20, 21). Previous findings convincingly demonstrate that the 5-HT$_{2A}$ receptor and the mGlu2 receptor form a specific heteromeric complex through which serotonin and glutamate ligands modulate the pattern of G protein coupling in living cells. We have also shown that the segment containing TM4 and TM5 of mGlu2 is necessary for this receptor to be assembled as a heterocomplex with the 5-HT$_{2A}$ receptor (13, 16). Despite this evidence, the specific residues at the heteromeric interface responsible for 5-HT$_{2A}$·mGlu2 receptor heterocomplex formation remain undefined. Similarly, the role of this GPCR heterocomplex in the psychosis-like behavioral responses induced in mice by hallucinogenic drugs has not been resolved.

Here, we show that three residues located at the intracellular end of TM4 of mGlu2 are necessary to form the 5-HT$_{2A}$·mGlu2 receptor heterocomplex in living cells. Based on these structural findings, we attempted to abolish the behavioral responses induced by hallucinogenic drugs in mice in which 5-HT$_{2A}$ and mGlu2 are co-expressed but are unable to form a complex. In addition, we provide evidence that the ligand binding interaction between 5-HT$_{2A}$ and mGlu2 as a receptor heterocomplex is dysregulated in the neocortex of schizophrenic subjects.

EXPERIMENTAL PROCEDURES

Drugs

1-(2,5-Dimethoxy-4-iodophenyl)-2-aminopropane (DOI) was purchased from Sigma. (1*R*,4*R*,5*S*,6*R*)-4-Amino-2-oxabicyclo [3.1.0]hexane-4,6-dicarboxylic acid (LY379268) was obtained from Tocris Cookson Inc. [^{3}H]Ketanserin was purchased from PerkinElmer Life Sciences, Inc. [^{3}H]2*S*-2-Amino-2-(1*S*,2*S*-2-carboxycyclopropan-1-yl)-3-(xanth-9-yl)-propionic acid ([^{3}H]LY341495) was purchased from American Radiolabeled Chemicals, Inc. All other chemicals were obtained from standard sources.

Transient Transfection of HEK293 Cells

Human embryonic kidney (HEK293) cells were maintained in Dulbecco's modified Eagle's medium supplemented with 10% (v/v) fetal bovine serum at 37 °C in a 5% CO_2-humidified atmosphere. Transfection was performed using Lipofectamine 2000 reagent (Invitrogen) according to the manufacturer's instructions.

Plasmid Construction

All PCRs were performed using Pfu Ultra Hotstart DNA polymerase (Stratagene) in a Mastercycler Ep Gradient Auto thermal cycler (Eppendorf). All the constructs were confirmed by DNA sequencing. Cycling conditions were 30 cycles of 94 °C for 30 s, 55 °C for 30 s, and 72 °C for 1 min/kb of amplicon, with an initial denaturation/activation of 94 °C for 2 min and a final extension of 72 °C for 7 min. The N-terminally c-Myc-tagged form of wild type human 5-HT$_{2A}$ (pcDNA3.1-c-Myc-5HT2A) and the N-terminally hemagglutinin (HA)-tagged forms of wild type human mGlu2 (pcDNA3.1-HA-mGlu2) and mGlu3 (pcDNA3.1-HA-mGlu3) have been described previously (13).

Chimeric Human mGlu2 with Transmembrane Domain 4 from Human mGlu3—The construct was generated by PCR-directed mutagenesis. Two overlapping PCR fragments were obtained using pcDNA3.1-HA-mGlu2 plasmid as a template and the primers hG2TM4/S (5′-AGTTCTCAGGTTTTCATCTGCCTGGGTCTGATCCTGGTGCAAATTGTGATGGTGTCTGTGTGGCTCATCGTGGAGGCACCGGGCACAGGCAAGGAGACAGCCC-3′) and hG2TM4/A (5′-GATGAGCCACACAGACACCATCACAATTTGCACCAGGATCAGACCCAGGCAGATGAAAACCTGAGAACTAGGACTGATGAAGCGTGGCCGCTGGGCACCCT-3′). The final amplification product (1058 bp), which includes the mutant sequence in the TM4 of the human mGlu3, was generated with outer oligonucleotides HpaI-hG2/S (5′-GCGGCCAGTTAACGGGCGCCGCCTC-3′) and BsrGI-hG2/A (5′-GGCTTCACCATGTACACCACCTGCA-3′). The final PCR product was digested using HpaI and BsrGI and subcloned into the same restriction sites of pcDNA3.1-HA-mGlu2.

Chimeric Human mGlu2 with Transmembrane Domain 5 from Human mGlu3

The plasmid was generated by PCR-directed mutagenesis. Two overlapping PCR fragments were obtained using pcDNA3.1-HA-mGlu2 plasmid as a template and the primers hG2TM5/S (5′-TCCAGCATGTTGATCTCTCTTACCTACGATGTGATCCTGGTGATCTTATGCACTGTGTACGCCTTCAAAACTCGCAAGTGCCCCGAAAACTT-3′) and hG2TM5/A (5′-TTTGAAGGCGTACACAGTGCATAAGATCACCAGGATCACATCGTAGGTAAGAGAGATCAACATGCTGGAATCGCGGTGGTTGCAGCGCAGTGTC-3′).

The final amplification product (1058 bp), which includes the mutant sequence in the TM5 of the human mGlu3, was generated with outer oligonucleotides HpaI-hG2/S and BsrGI-hG2/A (see above). The final PCR product was digested using HpaI and BsrGI and subcloned into the same restriction sites of pcDNA3.1-HA-mGlu2.

Chimeric Human mGlu3 with Transmembrane Domain 4 from Human mGlu2—The plasmid was generated by PCR-directed mutagenesis. Two overlapping PCR fragments were obtained using pcDNA3.1-HA-mGlu3 plasmid as a template and the primers hG3TM4/S (5′-GCCTCACAGGTGGCCATCTGCCTGGCACTTATCTCGGGCCAGCTGCTCATCGTGGTCGCCTGGCTGGTGCTGGAGGCCCCAGGCACCAGGAGGTATACC-3′) and hG3TM4/A (5′-CACCAGCCAGGCGACCACGATGAGCAGCTGGCCCGAGATAAGTGCCAGGCAGATGGCCACCTGTGAGGCGGGGCTGATGAATTTTGGCCTCTGAGCGCC-3′). The final amplification product (2640 bp), which includes the mutant sequence in the TM4 of the human mGlu2, was generated with outer primers NheI-hG3/S (5′-TTTTTGCTAGCATGAAGATGTTGACAAGACTGC-3′) and KpnI-hG3/A (5′-AAAAAGGTACCTCACAGAGATGAGGTGGTGGAGTC-3′). The final PCR product was digested using NheI and KpnI and subcloned into the same restriction sites of pcDNA3.1-HA-mGlu3.

Chimeric Human mGlu3 with Transmembrane Domain 5 from Human mGlu2—The plasmid was generated by PCR-directed mutagenesis. Two overlapping PCR fragments were obtained using pcDNA3.1-HA-mGlu3 plasmid as a template and the primers hG3TM5/S (5′-GCAAGTATGTTGGGCTCGCTGGCCTACAATGTGCTCCTCATCGCGCTCTGCACGCTTTATGCCTTCAAGACGCGGAAGTGCCCAGAAAATTTCAACGAAGC-3′) and hG3TM5/A (5′-CTTGAAGGCATAAAGCGTGCAGAGCGCGATGAGGAGCACATTGTAGGCCAGCGAGCCCAACATACTTGCATCTTTGACATTGCATTTTAGGATGAC-3′). The final amplification product (2640 bp), which includes the mutant sequence in the TM5 of the human mGlu2, was generated with outer primers NheI-hG3/S and KpnI-hG3/A (see above). The final PCR product was digested using NheI and KpnI and subcloned into the same restriction sites of pcDNA3.1-HA-mGlu3.

Chimeric Human mGlu2 with Intracellular End of Transmembrane Domain 4 from Human mGlu3—The plasmid was generated by PCR-directed mutagenesis. Two overlapping PCR fragments were obtained using pcDNA3.1-HA-mGlu2 plasmid as a template and the primers hG2TM4N/S (5′-AGTTCTCAGGTTTTCATCTGCCTGGGTCTTATCTCGGGCCAGCTGCTCATCG-3′) and hG2TM4N/A (5′-ACCCAGGCAGATGAAAACCTGAGAACTAGGACTGATGAAGCGTGGCCGC-3′). The final amplification product (1058 bp), which includes the mutant sequence in the intracellular end TM4 of the human mGlu3, was generated with outer oligonucleotides HpaI-hG2/S BsrGI-hG2/A (see above). The final PCR product was digested using HpaI and BsrGI and subcloned into the same restriction sites of pcDNA3.1-HA-mGlu2.

Introduction of single point mutations into human mGlu2—The mutants Ala-677S$^{4.40}$, Ala-681F$^{4.44}$, or Ala-685G$^{4.48}$ (single point mutations or combination of single point mutations) were constructed using the QuikChange II site-directed mutagenesis kit according to the manufacturer's protocol (Stratagene).

Co-immunoprecipitation Studies

Co-immunoprecipitation studies using N-terminally c-Myc-tagged form of 5-HT$_{2A}$ and N-terminally hemagglutinin (HA)-tagged forms of mGlu2, mGlu3, or mGlu2/mGlu3 chimeras in HEK293 were performed as described previously with minor modifications (13). Briefly, the samples were incubated overnight with protein A/G beads (Santa Cruz Biotechnology) and anti-c-Myc antibody (Cell Signaling Technology) at 4 °C on a rotating wheel. Equal amounts of proteins were resolved by SDS-PAGE. Detection of proteins by immunoblotting using anti-c-Myc and anti-HA antibodies (Cell Signaling Technology) was conducted using ECL system according to the manufacturer's recommendations.

Flow Cytometry-based Fluorescence Resonance Energy Transfer (FCM-based FRET)

Forms of mGlu2 and mGlu3 receptors C-terminally tagged with enhanced yellow fluorescent protein (eYFP) were described previously (13). Forms of chimeric mGlu2/mGlu3 receptors were C-terminally tagged with eYFP using a similar approach to that described above. The amplicon was PCR-amplified using the following primers: HindIII-hG2/S (5′-TTTTAAGCTTATGGTCCTTCTGTTGATCCT-3′) and KpnI-hG2/A (5′-TTTTGGTACCAAGCGATGACGTTGTCGAGT-3′) for chimeric mGlu2 forms and NheI-hG3/S (5′-TTTTGCTAGCATGGTCCTTCTGTTGATCCT-3′) and KpnI-hG3/A (5′-TTTTGGTACCCAGAGATGAGGTGGTGGAGT-3′) for chimeric mGlu3 forms. The PCR products were digested using HindIII and KpnI (chimeric mGlu2 forms) or NheI and KpnI (chimeric mGlu3 forms) and subcloned into the same restriction sites of pcDNA3.1-HA-mGlu2-eYFP or pcDNA3.1-HA-mGlu3-eYFP. To generate 5-HT$_{2A}$ receptor C-terminally tagged with monomeric red fluorescent protein (mCherry), the original mCherry was amplified by PCR from its original vector (Clontech) using the following primers: XbaI-mCherry/S (5′-TTTTTCTAGATTAGATGTTGTGGCGGATCT-3′) and NotI-mCherry/A (5′-TTTTGCGGCCGCATGGAGGACGGCAGCGTGCA-3′). The PCR product was digested using XbaI and NotI and subcloned into the same sites of pcDNA3.1-c-Myc-5HT2A-eCFP (13). Equivalent amounts of total DNA composed of a constant concentration of pcDNA3.1-c-Myc-5HT2A-mCherry and increasing concentrations of pcDNA3.1-c-Myc-mGlu2/m/Glu3-eYFP chimeras, together with empty pcDNA3.1 vector, were transfected. After 48 h, transfected HEK293 cells were gently washed in DMEM without phenol red, suspended to 500,000 cells/ml, and filtered through filter top tubes (35 μm) prior to FCM-based FRET assays. FCM-FRET measurements were performed using a flow cytometer equipped with 355-, 405-, 488-, and 532-nm lasers (LSR II, BD Biosciences). To measure eYFP and FRET, cells were excited with the 488-nm laser, fluorescence was collected in the eYFP channel with a standard 530/20 filter, and the FRET signal was measured with the 610/620 filter. To measure mCherry, cells were excited with the 532-nm laser, and the emission was also taken with a 610/620 filter. For each sample,

we evaluated a minimum of 50,000 positive cells that fell within the adjusted gate. All data were analyzed using the FlowJo software (Tree Star, Inc.). The fold change of FCM-based FRET was calculated as compared with the signal detected in cells co-transfected with the lowest ratio of eYFP-tagged mGlu2/mGlu3 chimera to 5-HT$_{2A}$-mCherry. FCM-based FRET signal obtained with the lowest ratio of eYFP-tagged mGlu2/mGlu3 chimera to 5-HT$_{2A}$-mCherry was not statistically different compared with that obtained with eYFP and 5-HT$_{2A}$-mCherry. Maximum FRET values (FRET$_{max}$) were calculated by nonlinear regression analysis.

Fluorescence Resonance Energy Transfer (FRET) Microscopy

Experiments were performed as reported previously (6, 13, 22). Briefly, cells were grown on poly-D-lysine-treated glass coverslips (number 0 thickness) and transfected to express the appropriate cerulean- and eYFP-tagged receptor fusion proteins. After 24 h, cells were placed into a microscope chamber containing physiological HEPES-buffered saline solution (130 mM NaCl, 5 mM KCl, 1 mM $CaCl_2$, 1 mM $MgCl_2$, 20 mM HEPES, and 10 mM D-glucose, pH 7.4). Cells were then imaged using a Zeiss Axio Observer.Z1 inverted microscope (Carl Zeiss), equipped with a ×63 (numerical aperture = 1.4), oil immersion Plan-Apochromat objective lens, and a photometrics Evolve 512 electron multiplying CCD camera (Roper Scientific, Trenton, NJ), coupled to a DualView 2 (DV2) image splitting device attached to the left-hand microscope port. The DV2 was fitted with the following Chroma (Chroma, Brattleboro, VT), ET series dichroic and emitters, so that FRET and donor intensity signals could be detected simultaneously without any potential threat of motion prior to the detection of the acceptor intensity signal as follows: ET t505LPXR dichroic, ET535/30m, and ET 470/24m. A computer-controlled Colibri LED excitation light source (Carl Zeiss), equipped with 425 and 505 nm LED modules, was used for rapid sequential excitation of experimental samples. Narrow band 427/10- nm and 504/12-nm excitation filters fitted to the front of the 425- and 505-nm LED modules, respectively, were used to produce 427- and 504-nm excitation light for the sequential excitation of cerulean- and eYFP-tagged receptors. Excitation light was reflected through the Plan-Apochromat lens using a cyan/yellow fluorescent protein dual band dichroic filter (Semrock; Rochester, NY, catalogue no. FF440/520-Di01) fitted to the 6-position reflector module turret. Using the multiple dimensional wavelength acquisition module of MetaMorph in combination with the image splitting device, FRET and donor intensity channel images were acquired simultaneously prior to the acquisition of the acceptor intensity channel image. 16 bit images were acquired without binning, and exposure time and camera gain were kept constant for all acquisitions taken during each experiment. Computer control of all electronic hardware and camera acquisition was achieved using Metamorph software (version 7.7.7, Molecular Devices, Sunnydale, CA).

A region of no fluorescence (*i.e.* black area) adjacent to the cell was used to determine the average background level of autofluorescence in the FRET, donor, and acceptor intensity channel images (* indicates background corrected channel images). Cell region *FRET intensity channel values were ratiometrically normalized to the amount of donor and acceptor fluorescent protein expressed to generate a final ratiometric value (FRET^R), which was dependent on receptor protein expression levels. A measurement cell region was defined on the *FRET intensity channel image and then transferred to the other channel images in exactly the same *x-y* position. Average fluorescence intensity values measured from each channel image cell region were then inserted into the following equation: FRET^R = *FRET channel cell region intensity/(*acceptor channel cell region intensity × a + (*donor channel cell region intensity × b), where a and b are the calculated cross-talk coefficient values (measured from cells expressing only donor or acceptor receptor fusion proteins), defining the amount of acceptor and donor cross-talk contamination in the recorded *FRET intensity channel. In the absence of fluorescence resonance energy transfer, FRET^R will have a predicted value of 1. FRET^R values greater than 1 indicate the occurrence of FRET. Quantified FRET^R values provided markedly better data quality compared with other ratiometric FRET metric algorithms (data not shown).

Molecular Modeling

Three-dimensional molecular models of the seven transmembrane domains of 5-HT$_{2A}$ and mGlu2 receptors were built using the crystal structures of β_2-adrenergic (Protein Data Bank code 2RH1) (23) receptor and rhodopsin (Protein Data Bank code 1F88) (24), respectively, as structural templates, and the homology-modeling program SWISS-MODEL (25). The use of the crystal structure of β_2-adrenergic receptor to build a model of a 5-HT$_{2A}$ receptor is justified by the sequence similarity between these two receptors (13). The suitability of the rhodopsin template to build models of family C GPCRs, which includes the mGlu2 receptor, has previously been discussed in the literature (26). The configuration deriving from atomic force microscopy of rhodopsin in native disk membranes (Protein Data Bank code 1N3M) (19) was used as a template for the heteromeric interface between 5-HT$_{2A}$ and mGlu2 receptors. This modeling was obtained with the assistance of PyMOL (27).

Experimental Animals

Experiments were performed on adult (8–12-week-old) male 129S6/Sv mice. 5-HT$_{2A}$-KO (*Htr2a*$^{-/-}$) mice have been previously described (28). mGlu2-KO (*Grm2*$^{-/-}$) mice were obtained from the RIKEN BioResource Center, Japan (29), and backcrossed for at least 10 generations onto 129S6/Sv background. All subjects were offspring of heterozygote breeding. For experiments involving genetically modified mice, wild type littermates were used as controls. Animals were housed at a 12-h light/dark cycle at 23 °C with food and water *ad libitum*. The Institutional Animal Use and Care Committee at Mount Sinai School of Medicine approved all experimental procedures.

Post-mortem Human Brain Tissue Samples

Human brains were obtained at autopsies performed in the Basque Institute of Legal Medicine, Bilbao, Spain, in compliance with policies of research and ethical boards for post-mortem brain studies between 1995 and 2008. Deaths were sub-

jected to retrospective searching for previous medical diagnosis and treatment using the examiner's information and records of hospitals and mental health centers. After searching of antemortem information was fulfilled, 27 subjects who had met criteria of schizophrenia according to the Diagnostic and Statistical Manual of Mental Disorders IV (30) were selected. A toxicological screening for antipsychotics, other drugs and ethanol was performed on blood, urine, liver and gastric contents samples. Subjects who gave negative results for antipsychotic drugs in the toxicological screening were considered antipsychotic-free at death. The toxicological assays were performed at the National Institute of Toxicology, Madrid, Spain, using a variety of standard procedures, including radioimmunoassay, enzymatic immunoassay, high performance liquid chromatography, and gas chromatography-mass spectrometry.

Controls for this study were chosen among the collected brains on the basis, whenever possible, of the following cumulative criteria: 1) negative medical information on the presence of neuropsychiatric disorders or drug abuse; 2) appropriate gender, age, post-mortem delay (time between death and autopsy), and freezing storage time to match each subject in the schizophrenia group; 3) sudden and unexpected death (*e.g.* motor vehicle accidents); and 4) toxicological screening for psychotropic drugs with negative results except for ethanol.

Specimens of prefrontal cortex (Brodmann's area 9) were dissected at autopsy (0.5–1 g of tissue) on an ice-cooled surface and immediately stored at −80 °C until use. The definitive pairs of antipsychotic-free schizophrenics, antipsychotic-treated schizophrenics, and respective matched controls are shown in Table 2. Pairs of schizophrenia and matched controls were processed simultaneously and under the same experimental conditions. Brain samples were assayed for pH and RNA integrity number as reported previously (see Table 2) (31).

Electron Microscopy

Experiments were performed as reported previously with minor modifications (32). Briefly, P8.5 mice were perfused with 2% paraformaldehyde, 2% glutaraldehyde in 0.1 M phosphate buffer, and blocks from frontal cortex were infiltrated with Lowicryl HM20 (Electron Microscopy Sciences) using a freeze substitution protocol. Ultrathin sections were collected on Formvar-coated nickel grids and immunolabeled with rabbit anti-5HT$_{2A}$ (Abcam, ab16028) and/or mouse anti-mGlu2 (Abcam, ab15672) antibodies. Labeling was visualized using donkey anti-rabbit 10-nm and anti-mouse 6-nm colloidal gold particles, respectively (both from Aurion). After labeling, sections were stained with 4% uranyl acetate (Sigma) and 1% phosphotungstic acid (Sigma). Digital images were taken on a Hitachi H7000 TEM at 80 kV with an Advanced Microscopy Techniques CCD camera.

Immunoblot Assays

Western blot assays in mouse brain samples were performed as reported previously (16, 33).

Radioligand Binding

Radioligand binding assays were performed as described previously with minor modifications (13). Briefly, cell pellets (HEK293 cells) or tissue samples (post-mortem human frontal cortex) were homogenized using a Teflon-glass grinder (10 up-and-down strokes at 1500 rpm) in 1 ml of binding buffer (see below), supplemented with 0.25 M sucrose. The crude homogenate was centrifuged at 1000 × *g* for 5 min at 4 °C, and the supernatant was re-centrifuged at 40,000 × *g* for 15 min at 4 °C. The resultant pellet (P_2 fraction) was washed twice in homogenization buffer and re-centrifuged in similar conditions. Aliquots were stored at −80 °C until assay. Protein concentration was determined using the Bio-Rad protein assay.

In HEK293 cells, [^{3}H]ketanserin binding was performed as reported previously with minor modifications (13). Competition curves were carried out by incubating DOI (10^{-12}–10^{-4} M; 18 concentrations) in binding buffer containing 4 nM [^{3}H]ketanserin. Nonspecific binding was determined in the presence of 10 μM methyl sergide (Tocris).

[^{3}H]LY341495 binding was performed as reported previously with minor modifications (13). In HEK293 cells, binding saturation curves were performed using 11 concentrations of [^{3}H]LY341495 binding (0.0625–20 nM). In post-mortem human prefrontal cortex, competition curves were carried out by incubating LY379268 (10^{-12}–10^{-4} M; 13 concentrations) in binding buffer containing 5 nM [^{3}H]LY341495. Experiments were performed in the presence and in the absence of 10 μM DOI. Nonspecific binding was determined in the presence of 1 mM L-glutamic acid (Tocris).

Virus-mediated Gene Transfer

The primers BamHI-hG2 (5′-TTTTGGATCCATGGTC-CTTCTGTTGATCC-3′) and XhoI-hG2 (5′-AAAACTC-GAGTCAAAGCGATGACGTTGTCG-3′) were used to amplify both sequences using the pcDNA3.1-HA-mGlu2 and the pcDNA3.1-HA-mGlu2ΔTM4N as templates, respectively. The PCR product (2658 bp) was digested using BamHI and XhoI and subcloned into the same restriction sites of a published bicistronic p1005+ herpes simplex virus (HSV) plasmid (33). Viral particles were then packaged as described before (33). HSV-mGlu2, HSV-mGlu2ΔTM4N, or control HSV-GFP was injected into the frontal cortex by stereotaxic surgery according to standard methods. Briefly, mice were anesthetized with a combination of ketamine (100 mg/kg) and xylazine (10 mg/kg) during the surgery. The virus was delivered bilaterally with a Hamilton syringe at a rate of 0.1 μl/min for a total volume of 0.5 μl on each side. The following coordinates were used: +1.6 mm rostral-caudal, −2.4 mm dorsal-ventral, and +2.6 mm medial-lateral from bregma (relative to dura) with a 10° lateral angle. The coordinates were taken according to a published atlas of the 129/Sv mouse strain (34). The Nissl staining of the coronal brain slice was taken from the mouse brain atlas with author's permission (Fig. 9*A*) (34). All experiments were performed 3–4 days after the viral infection when transgene expression is maximal (33). Virus-mediated mGlu2 and mGlu2-Δ-TM4N overexpression levels in the frontal cortex were confirmed by Western blotting and quantitative real time PCR (Fig. 9*B* and data not shown).

Immunohistochemistry

In HEK293 cells, experiments were performed as reported previously with minor modifications (35). Briefly, primary antibody anti-c-Myc (Cell Signaling Technology, catalog no. 2272) and anti-HA antibody (Cell Signaling Technology, catalog no. 2367) were added at dilutions 1:50 and incubated for 60 min at room temperature.

In mouse frontal cortex, experiments were performed as reported previously with minor modifications (16, 33). Briefly, GFP immunoreactivity was assayed by using polyclonal antibody (Santa Cruz Biotechnology sc-8334; 1:100) and Alexa 488 dye-conjugated anti-rabbit antibody (1:500).

Head-twitch Behavioral Response

Head-twitch experiments were performed as described previously (28).

Statistical Analysis

FCM-based FRET and radioligand binding data were analyzed using a nonlinear curve fitting software (GraphPad Prism). An extra-sum-of-squares (*F*-test) was used to determine statistical difference for simultaneous analysis of saturation and displacement curves. Statistical significance of biochemical or behavioral experiments involving three or more groups was assessed by one-way ANOVA followed by Bonferroni's post hoc test. Statistical significance of biochemical experiments involving two groups was assessed by Student's *t* test. The level of significance was chosen at $p = 0.05$. All data are presented as mean ± S.E.

RESULTS

Subcellular Co-localization of 5-HT$_{2A}$ and mGlu2 Receptors in Mouse Frontal Cortex—Frontal cortex integrates a wide array of functions in cognition and perception, and it has been recently implicated in schizophrenia and other psychotic disorders (13, 36, 37). Previous findings suggest that, as revealed by fluorescence microscopy in mouse frontal cortex, neurons positive for 5-HT$_{2A}$-like immunoreactivity are mostly also positive for mGlu2-like immunoreactivity (16). A similar overlap in the distribution of 5-HT$_{2A}$ and mGlu2 has been shown by radioactive autoradiography (38, 39) and fluorescent *in situ* hybridization (13) techniques. In studying GPCR heteromerization, it is important to validate a possible physical association between both receptors by determining their proximity and subcellular distribution in native tissue (40). Approaches such as the ones mentioned above, however, do not provide sufficient resolution to define proximity between 5-HT$_{2A}$ and mGlu2 receptors within individual cortical neurons. To explore the ultrastructural localization of 5-HT$_{2A}$ and mGlu2 receptors in neurons in the frontal cortex *in vivo*, we immunolabeled the receptors using different sized gold particles and visualized their distribution using electron microscopy. Labeling for 5-HT$_{2A}$ was observed most commonly in dendrites, near synapses, and extrasynaptically (Fig. 1*A* and data not shown). Labeling for mGlu2 was observed in presynaptic terminals and in dendrites at or near postsynaptic sites (Fig. 1*B* and data not shown). Both patterns are consistent with previous work in rat and monkey (41, 42). Notably, in double-immunolabeled sections, labeling for both receptors was observed in close proximity, particularly at or near synaptic junctions (Fig. 1*C*). The overall labeling patterns for the individual receptors in double-immunolabeled sections did not differ from that obtained in single immunolabeled sections (Fig. 1, *A*–*C*). Specificity of the primary antibodies against 5-HT$_{2A}$ and mGlu2 receptors was confirmed in knock-out (KO) mice (Fig. 1*D*). These data are consistent with a possible close proximity at subcellular levels between both receptors in frontal cortical neurons.

TM4 of mGlu2 Mediates Association with 5-HT$_{2A}$—We have previously shown a signaling cross-talk between 5-HT$_{2A}$ and mGlu2 receptors as a receptor heterocomplex that affects the pattern of G protein coupling *in vitro* in living cells (13, 16). Determining the structural components at the interaction interface responsible for stabilizing the quaternary structure of the 5-HT$_{2A}$·mGlu2 receptor heterocomplex is thus central to understanding its signaling function, yet such structural information remains rather limited. We first performed immunoprecipitation assays using anti-c-Myc antibodies in plasma membrane preparations of HEK293 cells transfected to express the c-Myc-tagged form of the 5-HT$_{2A}$ receptor alone or together with an HA-tagged form of the mGlu2 receptor or an equivalent HA-tagged form of the mGlu3 receptor. As reported previously (13), immunoprecipitation using anti-c-Myc antibodies in cells transfected to co-express the c-Myc-5-HT$_{2A}$ and HA-mGlu2 resulted in co-immunoprecipitation of anti-HA immunoreactivity (Fig. 2*A*). In SDS-polyacrylamide gels of such immunoprecipitated material, anti-HA immunoreactivity was detected as a mixture of a 95-kDa polypeptide and a band of ~190 kDa that corresponds to the size anticipated for an mGlu2 receptor homodimer (Fig. 2*A*). Co-immunoprecipitation of anti-HA immunoreactivity was not produced when either c-Myc-5-HT$_{2A}$ or HA-mGlu2 was expressed individually, or when plasma membrane preparations expressing either the c-Myc- or the HA-tagged forms of the receptors were combined before immunoprecipitation (Fig. 2*A*). More importantly, co-immunoprecipitation of anti-HA immunoreactivity was not produced when c-Myc-5-HT$_{2A}$ and HA-mGlu3 were co-expressed (Fig. 2*A*). Such observations are consistent with receptor protein complex formation between the co-expressed, tagged forms of c-Myc-5-HT$_{2A}$ and HA-mGlu2, but not HA-mGlu3, receptors.

The differences in the capacity of mGlu2 and mGlu3 receptors to interact with the 5-HT$_{2A}$ receptor provided the basis of our strategy to identify the structural components at the interaction interface responsible for 5-HT$_{2A}$·mGlu2 receptor heterocomplex formation. Using a series of molecular chimeras of mGlu2 and mGlu3, we have previously demonstrated that the segment containing TM4 and TM5 of mGlu2 is necessary for 5-HT$_{2A}$·mGlu2 receptor heterocomplex formation (13). We found here that the HA-tagged form of the mGlu2 receptor chimera containing the segment corresponding to TM4 of the mGlu3 receptor (mGlu2ΔTM4) did not show evidence of being able to co-immunoprecipitate with the c-Myc-tagged form of the 5-HT$_{2A}$ receptor (Fig. 2*B*). On the contrary, HA-mGlu2ΔTM5 was capable of co-immunoprecipitating with c-Myc-5-HT$_{2A}$ (Fig. 2*B*). Analysis of HA-mGlu3ΔTM4

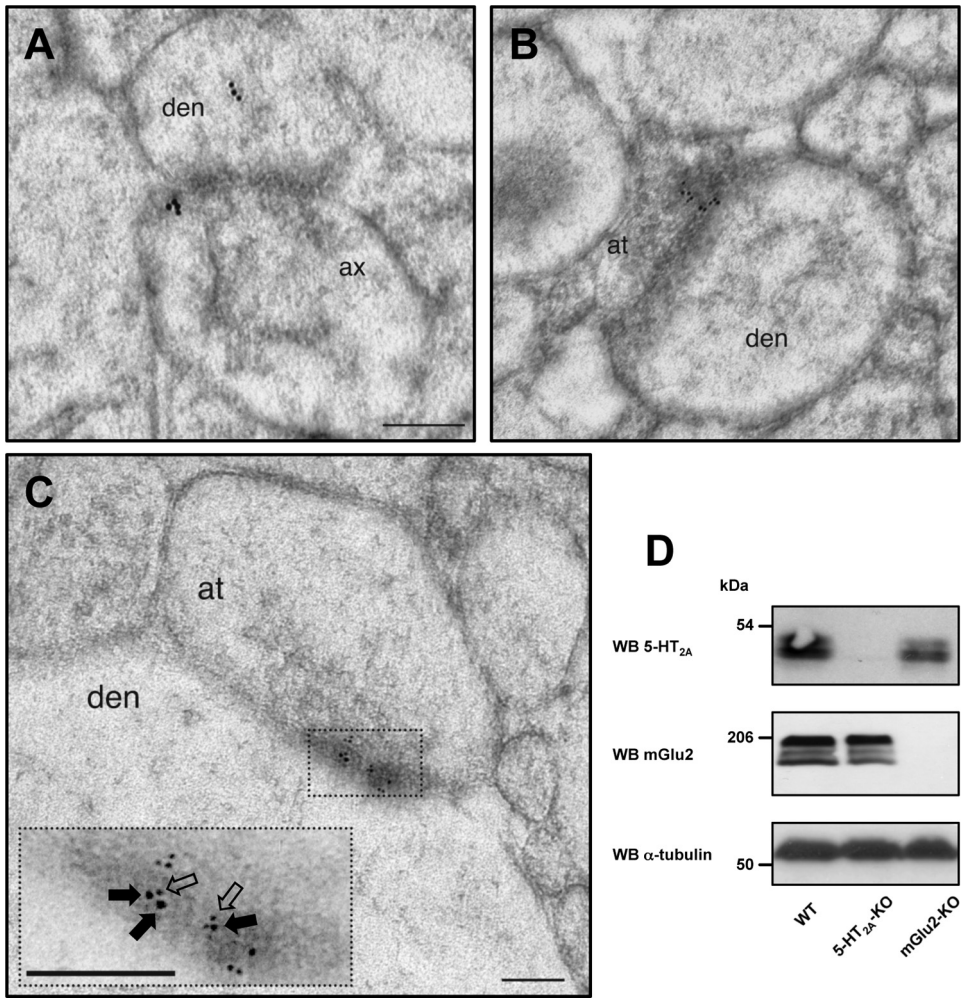

FIGURE 1. **Subcellular co-localization of 5-HT$_{2A}$ and mGlu2 receptors in mouse cortical neurons.** *A,* immunogold labeling for the 5-HT$_{2A}$ receptor. *B,* immunogold labeling for the mGlu2 receptor. *C,* immunogold labeling for 5-HT$_{2A}$ and mGlu2 receptors. Different sized *black dots* show 5-HT$_{2A}$ receptor immunolabeling (larger 10-nm gold particles) and mGlu2 receptor immunolabeling (smaller 6-nm gold particles). *Inset*, high magnification view of region delineated by *boxed area*. Note that the 10-nm gold particles (*filled arrows*) and the 6-nm gold particles (*open arrows*) are located in very close proximity at synaptic junctions in mouse frontal cortex (*den*, dendrite; *ax*, axon; *at*, axon terminal). *Scale bars,* 100 nm. *D,* Western blots (*WB*) in frontal cortex of wild type (*WT*), 5-HT$_{2A}$-KO, and mGlu2-KO mice. Representative immunoblots in plasma membrane preparations of mouse frontal cortex are shown.

and HA-mGlu3ΔTM5 showed that TM4 of mGlu2 rescues heterocomplex formation with c-Myc-5-HT$_{2A}$, whereas TM5 of mGlu2 is not significantly involved (Fig. 2*C*). Together, these data suggest that TM4 of mGlu2 is necessary to form a protein complex with the 5-HT$_{2A}$ receptor.

Intracellular End of TM4 Mediates Association with 5-HT$_{2A}$—We next went on to investigate the residues in TM4 of mGlu2 that are principally responsible for heteromeric formation. In homomers of family A GPCRs, some studies have proposed a critical role for the residues located near the intracellular end of TM4 (6, 19). However, molecular proximity between a subset of residues along the entire length of TM4 has also been observed (43). To address this question directly, we substituted residues of TM4 based on inferences from primary sequence comparisons between mGlu2 and mGlu3 receptors (Fig. 3*A*). We found that substitution of residues Ala-677$^{4.40}$, Ala-681$^{4.44}$, and Ala-685$^{4.48}$ in mGlu2 for Ser-686$^{4.40}$, Phe-690$^{4.44}$, and Gly-694$^{4.48}$ in mGlu3 (HA-mGlu2ΔTM4N) significantly reduces co-immunoprecipitation with c-Myc-5-HT$_{2A}$ (Fig. 3, *B* and *C*) (superscripts in this form indicate Ballesteros-Weinstein numbering for conserved GPCR residues) (44). The central importance of Ala-677$^{4.40}$, Ala-681$^{4.44}$, and Ala-685$^{4.48}$ in TM4 of HA-mGlu2 was further supported by the absence of observable effect of substitutions at positions Ser-688$^{4.51}$, Gly-689$^{4.52}$, Leu-691$^{4.54}$, Leu-692$^{4.55}$, Ile-693$^{4.56}$, Val-695$^{4.58}$, Ala-696$^{4.59}$ and Val-699$^{4.62}$ in mGlu2 for Leu-697$^{4.51}$, Val-698$^{4.52}$, Ile-700$^{4.54}$, Val-701$^{4.55}$, Met-702$^{4.56}$, Ser-704$^{4.58}$, Val-705$^{4.59}$, and Ile-708$^{4.62}$ in mGlu3 (HA-mGlu2ΔTM4C) in co-immunoprecipitation assays with c-Myc-5-HT$_{2A}$ (Fig. 3, *B* and *C*). Nevertheless, findings based on co-immunoprecipitation assays do not exclude the possibility that 5-HT$_{2A}$ and mGlu2 receptors interact indirectly, via scaffolding proteins, as part of the same protein complex, rather than in close molecular proximity as a GPCR heteromeric complex (45). We therefore attempted to validate our observations that Ala-677$^{4.40}$, Ala-681$^{4.44}$, and Ala-685$^{4.48}$ of mGlu2 are responsible for GPCR heteromeric formation with the 5-HT$_{2A}$ receptor.

Flow cytometry (FCM) is a noninvasive approach that allows quantitative determination of the fluorescence signal from individual cells in a large population (46). Fluorescence reso-

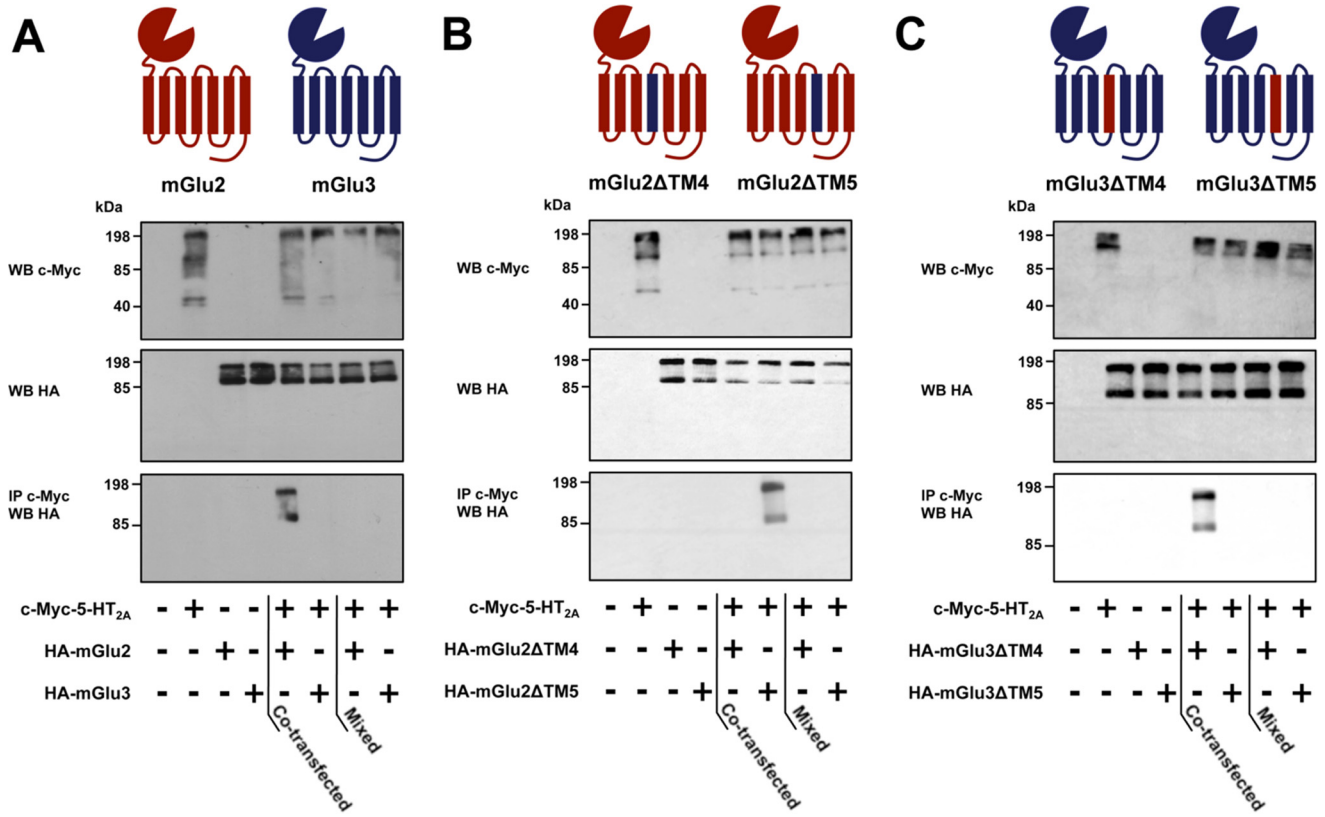

FIGURE 2. **TM4 of mGlu2 mediates complex formation with the 5-HT$_{2A}$ receptor.** *A,* co-immunoprecipitation (*IP*) experiments of c-Myc-5-HT$_{2A}$ and HA-mGlu2 or HA-mGlu3 in co-transfected HEK293 cells. The mGlu2, but not the mGlu3, co-immunoprecipitates with the 5-HT$_{2A}$ receptor. *B,* co-immunoprecipitation experiments of c-Myc-5-HT$_{2A}$ and HA-mGlu2ΔTM4 or HA-mGlu2ΔTM5 in co-transfected HEK293 cells. The presence of TM4, but not TM5, of the mGlu2 receptor is necessary to co-immunoprecipitate with the 5-HT$_{2A}$ receptor. *C,* co-immunoprecipitation experiments of c-Myc-5-HT$_{2A}$ and HA-mGlu3ΔTM4 or HA-mGlu3ΔTM5 in co-transfected HEK293 cells. The presence of TM4, but not TM5, of the mGlu2 conferred the capacity to co-immunoprecipitate with the 5-HT$_{2A}$ receptor. Schematic of mGlu2/mGlu3 chimeras studied are shown. For a control, cells separately expressing the c-Myc- or HA-tagged forms were mixed. Similar findings were obtained in two other independent experiments. *WB,* Western blot.

nance energy transfer (FRET) between donor and acceptor fluorophores fused to distinct GPCRs occurs only when the FRET partners are located within 100 Å of each other, a distance that falls within the dimensions anticipated for GPCR homo- and heteromers (47). We combined FRET and FCM approaches (FCM-based FRET) to study receptor interactions in individual intact living cells (46). To establish an assay to measure FRET by FCM, we first performed FRET titration experiments with cells co-expressing increasing amounts of the enhanced yellow fluorescent protein (eYFP)-tagged mGlu2 receptor (mGlu2-eYFP) as a donor and constant amounts of the cherry fluorescent protein (mCherry)-tagged 5-HT$_{2A}$ receptor (5-HT$_{2A}$-mCherry) as an acceptor (Fig. 4*A*). Linear *versus* nonlinear regression analysis showed that FRET signal in cells co-expressing mGlu2-eYFP and 5-HT$_{2A}$-mCherry can be fit preferably by a saturation curve (Fig. 4*B*). One of the main limitations of the FRET assay is that the signal may result from random collision of the labeled proteins (48). Our findings indicate that linear regression provided the best fit to FRET signal in cells co-transfected with mGlu3-eYFP and 5-HT$_{2A}$-mCherry. Similar findings were obtained with the fluorescent protein eYFP and 5-HT$_{2A}$-mCherry (Fig. 4*B*). Analysis of the maximum FRET values (FRET$_{max}$) also showed lower signal between mGlu3-eYFP or eYFP and 5-HT$_{2A}$-mCherry as compared with mGlu2-eYFP and 5-HT$_{2A}$-mCherry (Fig. 4*C*). These results support the sensitivity and specificity of the FCM-based FRET assay in HEK293 cells. They also indicate that mGlu2-eYFP and 5-HT$_{2A}$-mCherry maintain close molecular proximity, whereas the FRET signal between mGlu3-eYFP and 5-HT$_{2A}$-mCherry results from random collision as it is not significantly different from that obtained in cells co-expressing the isolated fluorescent protein eYFP and 5-HT$_{2A}$-mCherry.

To validate further the central importance of Ala-677$^{4.40}$, Ala-681$^{4.44}$, and Ala-685$^{4.48}$ of mGlu2 in forming the GPCR heteromeric interface with the 5-HT$_{2A}$ receptor, and to support the specificity of the FCM-based FRET assay, we carried out additional experiments with mGlu2ΔTM4N and mGlu2ΔTM4C in living cells. Notably, FRET titration experiments showed that co-expression of mGlu2ΔTM4N-eYFP and 5-HT$_{2A}$-mCherry resulted in undetectable levels of FRET signal (Fig. 5*A*), whereas a saturable FRET signal similar to that obtained in cells co-expressing mGlu2-eYFP and 5-HT$_{2A}$-mCherry was obtained between mGlu2ΔTM4C-eYFP and 5-HT$_{2A}$-mCherry (Fig. 5*A*; see also Fig. 5*B* for FRET$_{max}$ values).

To confirm the specificity of these interactions, and to rule out a role of donor/acceptor orientation, we performed FRET microscopy experiments in living cells with the use of the cerulean fluorescent protein-tagged 5-HT$_{2A}$ receptor (5-HT$_{2A}$-cerulean) as donor and eYFP-tagged mGlu2/mGlu3 chimeras as acceptors (Fig. 5*C*). The FRET signal

A

Species	Accession	4.40	TM4
GRM2 *(Homo sapiens)*	NP_000830	677	ASQVAICLALISGQLLIVVAWLV
GRM2 *(Mus musculus)*	NP_001153825	677	ASQVAICLALISGQLLIVAAWLV
GRM2 *(Rattus norvegicus)*	NP_001099181	677	ASQVAICLALISGQLLIVAAWLV
GRM2 *(Pan troglodytes)*	BAI22787	677	ASQVAICLALISGGLLIVVAWLV
GRM2 *(Bos taurus)*	NP_001192795	677	ASQVAICLALISGGLLIVATWLV
GRM3 *(Homo sapiens)*	NP_000831	686	SSQVFICLGLILVQIVMVSVWLI
GRM3 *(Mus musculus)*	NP_862898	686	SSQVFICLGLILVQIVMVSVWLI
GRM3 *(Rattus norvegicus)*	NP_001099182	686	SSQVFICLGLILVQIVMVSVWLI
GRM3 *(Macaca fascicularis)*	ABD74419	686	SSQVFICLGLILVQIVMVSVWLI
GRM3 *(Bos taurus)*	NP_001091592	686	SSQVFICLGLILVQIVVVSVWLI

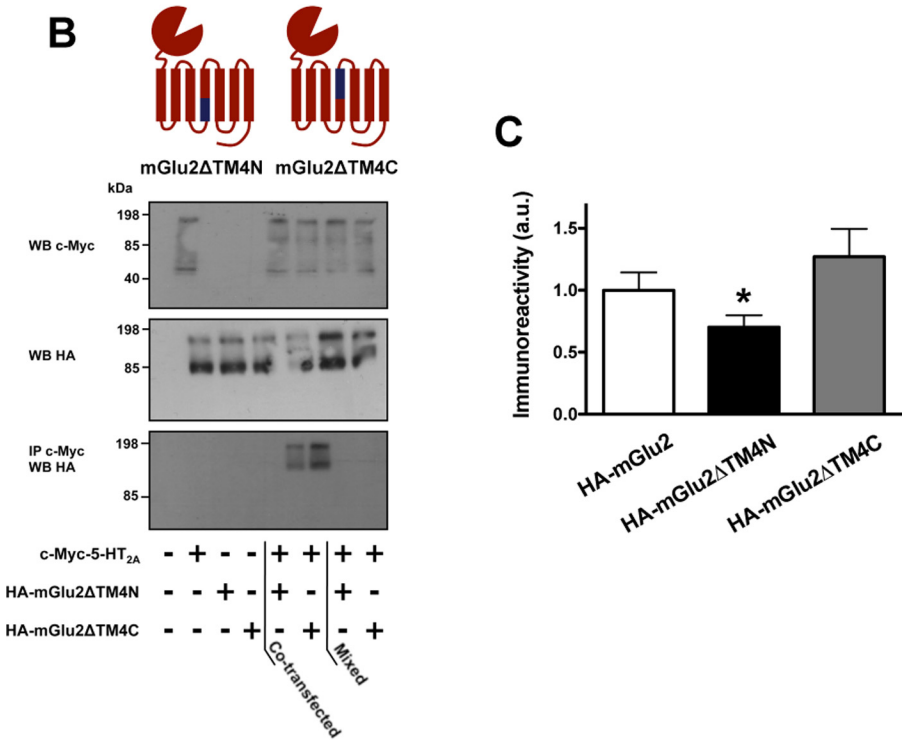

FIGURE 3. **Intracellular end of TM4 of mGlu2 mediates complex formation with the 5-HT$_{2A}$ receptor.** *A,* multiple sequence alignment of the transmembrane domain 4 (*TM4*) of mGlu2 (*GRM2*) and mGlu3 (*GRM3*) receptors. All residues were identified by the Ballesteros-Weinstein numbering system (*i.e.* the most conserved residue in the TM in which they are located is assigned the position index "50"), as well as by the residue numbers of the amino acid sequences in the species shown. Residues that are different between mGlu2 and mGlu3 receptors are highlighted in *red*. *B,* co-immunoprecipitation (*IP*) experiments of c-Myc-5-HT$_{2A}$ and HA-mGlu2ΔTM4N or HA-mGlu2ΔTM4C in co-transfected HEK293 cells. The presence of the intracellular end of TM4, but not the extracellular end of TM4, of the mGlu2 receptor is necessary to co-immunoprecipitate with the 5-HT$_{2A}$ receptor. Schematic of mGlu2/mGlu3 chimeras studied are shown. For a control, cells separately expressing the c-Myc- or HA-tagged forms were mixed. Similar findings were obtained in two other independent experiments. *WB*, Western blot. *C,* co-immunoprecipitation experiments of c-Myc-5-HT$_{2A}$ and HA-mGlu2, HA-mGlu2ΔTM4N, or HA-mGlu2ΔTM4C in co-transfected HEK293 cells. Co-immunoprecipitation was decreased by substitution of residues Ala-677$^{4.40}$, Ala-681$^{4.44}$, and Ala-685$^{4.48}$ in mGlu2 for Ser-686$^{4.40}$, Phe-690$^{4.44}$, and Gly-694$^{4.48}$ in mGlu3 (HA-mGlu2ΔTM4N), but not by substitution of residues Ser-688$^{4.51}$, Gly-689$^{4.52}$, Leu-691$^{4.54}$, Leu-692$^{4.55}$, Ile-693$^{4.56}$, Val-695$^{4.58}$, Ala-696$^{4.59}$, and Val-699$^{4.62}$ in mGlu2 for Leu-697$^{4.51}$, Val-698$^{4.52}$, Ile-700$^{4.54}$, Val-701$^{4.55}$, Met-702$^{4.56}$, Ser-704$^{4.58}$, Val-705$^{4.59}$, and Ile-708$^{4.62}$ in mGlu3 (HA-mGlu2ΔTM4C), as compared with HA-mGlu2 ($n = 9$). *, $p < 0.05$; Bonferroni's post hoc test of one-way ANOVA. *Error bars* represent S.E.

between 5-HT$_{2A}$-cerulean and mGlu2ΔTM4C-eYFP was similar to that obtained with 5-HT$_{2A}$-cerulean and mGlu2-eYFP, whereas co-expression of 5-HT$_{2A}$-cerulean and mGlu2ΔTM4N-eYFP resulted in a signal that was reduced close to the value observed with co-expression of 5-HT$_{2A}$-cerulean and mGlu3-eYFP (Fig. 5, *C* and *D*).

We next explored the contribution of individual residues at the cytoplasmic end of TM4 of the mGlu2 receptor in GPCR heteromeric complex formation with the 5-HT$_{2A}$ receptor. We performed FCM-based FRET measurements using mGlu2-eYFP with single point mutations at Ala-677$^{4.40}$, Ala-681$^{4.44}$, or Ala-685$^{4.48}$ to the corresponding residues from the mGlu3 receptor and 5-HT$_{2A}$-mCherry. As stated above, FCM-based FRET signal in cells co-expressing mGlu2-eYFP and 5-HT$_{2A}$-mCherry can be fit preferably by a saturation curve (Fig. 6*A*). The simultaneous analysis of multiple titration curves indicated that A681F$^{4.44}$ or A685G$^{4.48}$, but not A677S$^{4.40}$, significantly affected the FRET saturation curves as compared with mGlu2-eYFP (Fig. 6*A*). More importantly, analysis of individual FRET$_{max}$ values showed increased signal of A677S$^{4.40}$, A681F$^{4.44}$, and A685G$^{4.48}$ as compared with mGlu3-eYFP (Fig. 6*B*). This suggests that two or more of these three residues are necessary at the heteromeric interface between 5-HT$_{2A}$ and mGlu2 receptors.

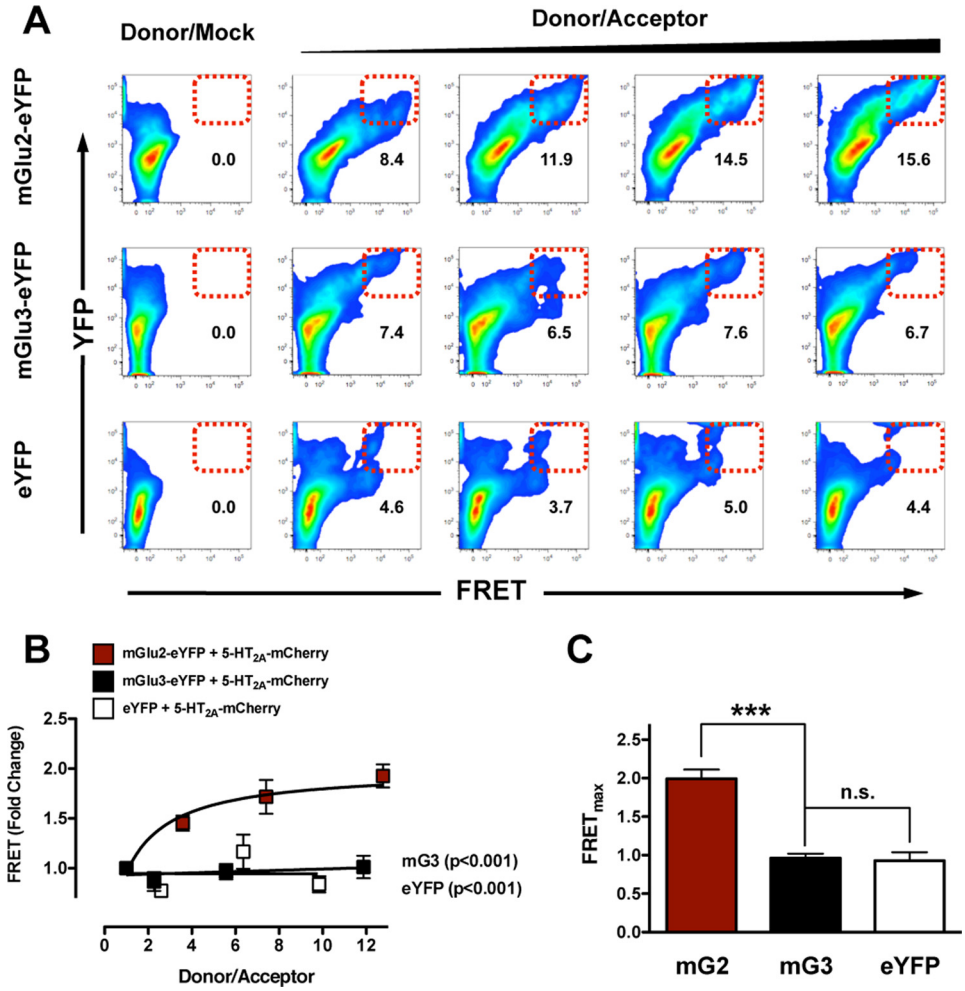

FIGURE 4. **Measurement of molecular interactions between 5-HT$_{2A}$ and mGlu2 receptors by FCM-based FRET assay.** *A,* representative flow-cytometric analysis of FRET between mGlu2-eYFP (*donor*) and 5-HT$_{2A}$-mCherry (*acceptor*). Increasing amounts of mGlu2-eYFP were co-expressed with a constant amount of 5-HT$_{2A}$-mCherry in HEK293 cells. The specificity of mGlu2-eYFP and 5-HT$_{2A}$-mCherry interactions was assessed by comparison with co-expression of mGlu3-eYFP and 5-HT$_{2A}$-mCherry, and eYFP and 5-HT$_{2A}$-mCherry. The *red boxes* outline the gate in which FRET signal was seen. *Numbers* represent percentage of cells within the indicated gates. *B,* fold change of FCM-based FRET signal for each combination of eYFP- or mCherry-tagged receptors. Only the data obtained in cells co-expressing mGlu2-eYFP and 5-HT$_{2A}$-mCherry can be fit preferably by a saturation curve, assessed by *F* test. The other co-transfection datasets show linear correlations (n = 3–8). Note that mGlu3 or eYFP decrease the FCM-based FRET signal as compared with mGlu2: mGlu2-eYFP + 5-HT$_{2A}$-mCherry compared with eYFP + 5-HT$_{2A}$-mCherry, $F(2,37) = 21.58$, $p < 0.001$; mGlu2-eYFP + 5-HT$_{2A}$-mCherry compared with mGlu3-eYFP + 5-HT$_{2A}$-mCherry, $F(2,41) = 27.96$, $p < 0.001$. *C,* FRET$_{max}$ obtained from individual FCM-based FRET saturation curves. ***, $p < 0.001$; *n.s.,* not significant; Bonferroni's post hoc test of one-way ANOVA. *Error bars* represent S.E.

We therefore introduced each of the double mutations into mGlu2-eYFP (A677S$^{4.40}$ and A681F$^{4.44}$, A677S$^{4.40}$ and A685G$^{4.48}$, or A681F$^{4.44}$ and A685G$^{4.48}$). Notably, we found that the FCM-based FRET signal between each of these double mutants and 5-HT$_{2A}$-mCherry did not differ significantly from the one obtained between mGlu3-eYFP and 5-HT$_{2A}$-mCherry (Fig. 6, *C* and *D*). The levels of expression of wild type and mutant heterologous constructs, as determined by [^{3}H]ketanserin and [^{3}H]LY341495 binding saturation curves, were comparable (c-Myc-5-HT$_{2A}$: B_{max}, 706.7 ± 165.6 fmol/mg protein, and K_D, 7.1 ± 2.9 nM; 5-HT$_{2A}$-mCherry: B_{max}, 732.1 ± 93.5 fmol/mg protein, and K_D, 5.2 ± 1.4 nM; HA-mGlu2: B_{max}, 1808 ± 70.1 fmol/mg protein, and K_D, 3.1 ± 0.4 nM; HA-mGlu3: B_{max}, 3981 ± 173.1 fmol/mg protein, and K_D, 6.8 ± 0.8 nM; mGlu2ΔTM4: B_{max}, 1914 ± 134.5 fmol/mg protein, and K_D, 3.7 ± 0.8 nM; mGlu2ΔTM5: B_{max}, 2550 ± 122.4 fmol/mg protein, and K_D, 2.3 ± 0.4 nM; mGlu3ΔTM4: B_{max}, 2894 ± 143.7 fmol/mg protein, and K_D, 4.5 ± 0.6 nM; mGlu3ΔTM5: B_{max}, 2662 ± 62.2 fmol/mg protein, and K_D, 3.4 ± 0.2 nM; mGlu2ΔTM4N: B_{max}, 1331 ± 67.7 fmol/mg protein, and K_D, 4.8 ± 0.7 nM; mGlu2ΔTM4C: B_{max}, 1344 ± 56.4 fmol/mg protein, and K_D, 3.0 ± 0.4 nM; mGlu2-A677S$^{4.40}$: B_{max}, 2113 ± 142.8 fmol/mg protein, and K_D, 4.7 ± 0.9 nM; mGlu2-A681F$^{4.44}$: B_{max}, 1337 ± 73.6 fmol/mg protein, and K_D, 2.6 ± 0.5 nM; mGlu2-A685G$^{4.48}$: B_{max}, 930.1 ± 35.5 fmol/mg protein, and K_D, 2.8 ± 0.3 nM; mGlu2-A677S$^{4.40}$/A681F$^{4.44}$: B_{max}, 2406 ± 48.7 fmol/mg protein, and K_D, 4.6 ± 0.2 nM; mGlu2-A677S$^{4.40}$/A685G$^{4.48}$: B_{max}, 2688 ± 54.9 fmol/mg protein, and K_D, 5.0 ± 0.3 nM; mGlu2-A681F$^{4.44}$/A685G$^{4.48}$: B_{max}, 3456 ± 184.9 fmol/mg protein, and K_D, 7.2 ± 1.0 nM (n = 2 per group). Immunocytochemistry assays demonstrated evidence of plasma membrane expression of N-terminally c-Myc-tagged 5-HT$_{2A}$, and N-terminally tagged mGlu2, mGlu3, and mGlu2/mGlu3 chimeras in HEK293 cells (data not shown). Taken together, our findings indicate that any two of the three residues located at the intracellular end of TM4, which, based on a receptor

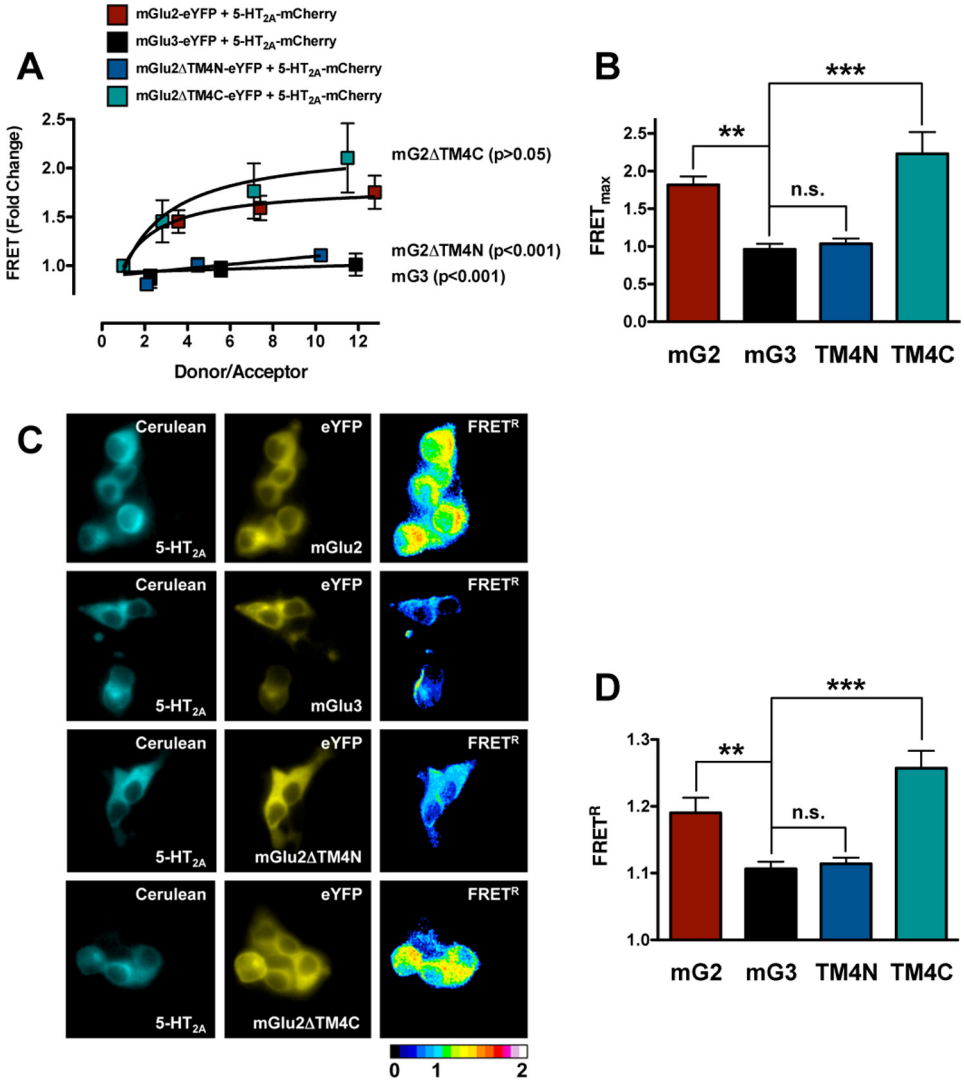

FIGURE 5. **Three residues located at the intracellular end of TM4 of mGlu2 mediate complex formation with the 5-HT$_{2A}$ receptor.** *A,* fold change of FCM-based FRET signal for each combination of eYFP- or mCherry-tagged receptors (eYFP-tagged, *donor*; mCherry-tagged, *acceptor*). Data obtained in cells co-expressing mGlu2-eYFP and 5-HT$_{2A}$-mCherry or mGlu2ΔTM4C-eYFP and 5-HT$_{2A}$-mCherry can be fit preferably by a saturation curve, assessed by *F* test. Data obtained in cells co-expressing mGlu3-eYFP and 5-HT$_{2A}$-mCherry or mGlu2ΔTM4N-eYFP and 5-HT$_{2A}$-mCherry show linear correlations ($n = 4$). Note that mGlu2ΔTM4N or mGlu3, but not mGlu2ΔTM4C, decreases the FCM-based FRET signal as compared with mGlu2: mGlu2-eYFP + 5-HT$_{2A}$-mCherry compared with mGlu3-eYFP + 5-HT$_{2A}$-mCherry, $F(2,28) = 29.09$, $p < 0.001$; mGlu2-eYFP + 5-HT$_{2A}$-mCherry compared with mGlu2ΔTM4N-eYFP + 5-HT$_{2A}$-mCherry, $F(2,28) = 25.21$, $p < 0.001$; mGlu2-eYFP + 5-HT$_{2A}$-mCherry compared with mGlu2ΔTM4C-eYFP + 5-HT$_{2A}$-mCherry, $F(2,28) = 1.23$, $p > 0.05$. *B,* FRET$_{max}$ obtained from individual FCM-based FRET saturation curves. **, $p < 0.01$; ***, $p < 0.001$; *n.s*, not significant; Bonferroni's post hoc test of one-way ANOVA. *C,* single-cell FRET in live HEK293 cells co-expressing 5-HT$_{2A}$-cerulean and either mGlu2, mGlu3, mGlu2ΔTM4N, or mGlu2ΔTM4C chimera, all tagged with eYFP (cerulean-tagged, *donor*; eYFP-tagged, *acceptor*). Pseudo-color images of FRET signals represent the ratiometric normalization of the FRET signal (FRET^R). *D,* results from a single experiment, representative of three independent studies, are shown. 5-HT$_{2A}$-cerulean + mGlu2-eYFP ($n = 23$); 5-HT$_{2A}$-cerulean + mGlu3-eYFP ($n = 16$); 5-HT$_{2A}$-cerulean + mGlu2ΔTM4N-eYFP ($n = 21$); 5-HT$_{2A}$-cerulean + mGlu2ΔTM4C-eYFP ($n = 21$). Significant increases in FRET^N signal over control are seen only with co-expression of 5-HT$_{2A}$ and either mGlu2 or mGlu2ΔTM4C. **, $p < 0.01$; ***, $p < 0.001$; *n.s.,* not significant; Bonferroni's post hoc test of one-way ANOVA. *Error bars* represent S.E.

model face outwards (Fig. 7, *A* and *B*), are responsible for the dramatic difference in heteromer formation between the 5-HT$_{2A}$ receptor and mGlu2 or mGlu3 receptors in living cells.

Ala-677$^{4.40}$, Ala-681$^{4.44}$, and Ala-685$^{4.48}$ of mGlu2 Affect the Allosteric Cross-talk between mGlu2 and 5-HT$_{2A}$ Receptors—Competition binding assays can provide a sensitive measure of functional interactions within a receptor heterocomplex (49). To determine whether Ala-677$^{4.40}$, Ala-681$^{4.44}$, and Ala-685$^{4.48}$ of mGlu2 have functional roles in heteromer pharmacology, we examined the effects of co-expressed A677S$^{4.40}$, A681F$^{4.44}$, and A685G$^{4.48}$ on the competition binding displacement curves of the 5-HT$_{2A}$ receptor antagonist [^{3}H]ketanserin by the 5-HT$_{2A}$ receptor agonist DOI. As expected, competition binding experiments of [^{3}H]ketanserin by DOI were best described by a two-site model in cells expressing the 5-HT$_{2A}$ receptor alone (Fig. 8*A* and Table 1). Displacement of [^{3}H]ketanserin binding by DOI became monophasic in cells co-expressing 5-HT$_{2A}$ and mGlu2, but not mGlu3, receptors (Fig. 8*A* and Table 1). We also demonstrate that A677S$^{4.40}$, A681F$^{4.44}$, and A685G$^{4.48}$ together (mGlu2ΔTM4N) (Fig. 8*B* and Table 1), or any combination of two of these three alterations (Fig. 8*C* and Table 1), do not affect the fit to a two-site model of DOI displacing [^{3}H]ketanserin binding, as compared with that observed with the 5-HT$_{2A}$ receptor alone (see Fig. 8*A*).

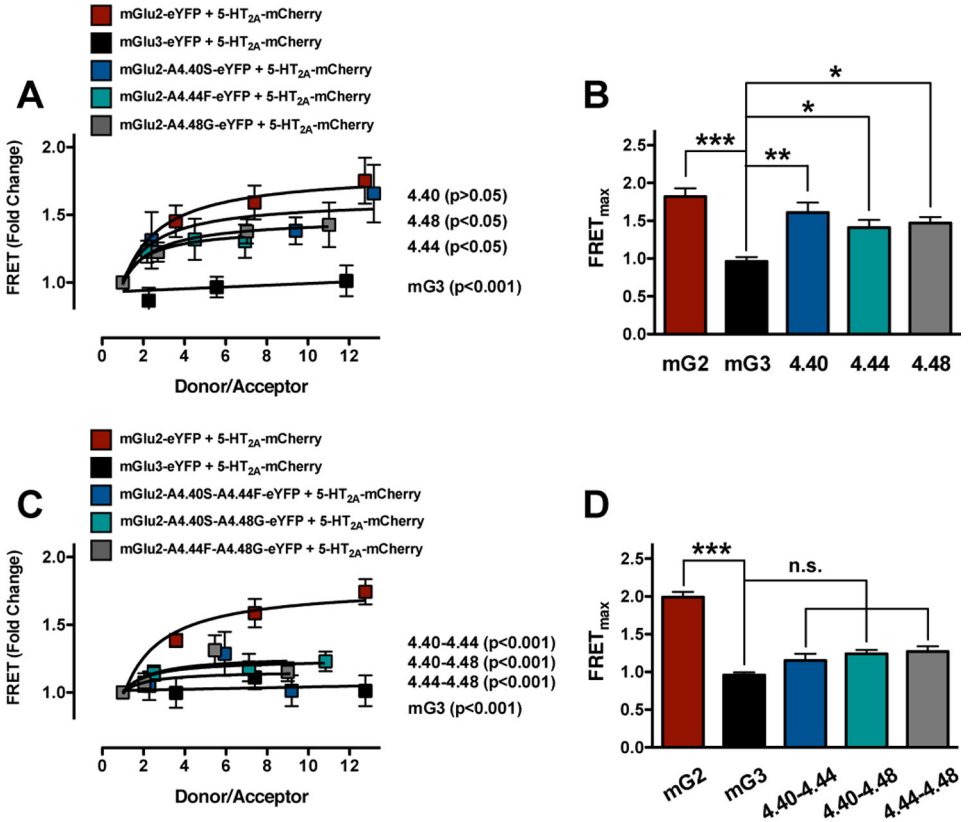

FIGURE 6. **Any two of the three residues located at the intracellular end of TM4 of mGlu2 mediate complex formation with the 5-HT$_{2A}$ receptor.** *A,* fold change of FCM-based FRET signal for each combination of eYFP- or mCherry-tagged receptors (eYFP-tagged, *donor*; mCherry-tagged, *acceptor*). Data obtained in cells co-expressing either mGlu2, mGlu3, mGlu2-A677S$^{4.40}$, mGlu2-A681F$^{4.44}$, or mGlu2-A685G$^{4.48}$, all tagged with eYFP, and 5-HT$_{2A}$-cerulean can be fit preferably by a saturation curve, assessed by *F* test. Data obtained in cells co-expressing mGlu3-eYFP and 5-HT$_{2A}$-mCherry show linear correlations ($n = 4–8$). Note that mGlu2-A681F$^{4.44}$, mGlu2-A685G$^{4.48}$, or mGlu3, but not mGlu2-A677S$^{4.40}$, decrease the FCM-based FRET signal as compared with mGlu2: mGlu2-eYFP + 5-HT$_{2A}$-mCherry compared with mGlu3-eYFP + 5-HT$_{2A}$-mCherry, $F(2,40) = 40.17$, $p < 0.001$; mGlu2-eYFP + 5-HT$_{2A}$-mCherry compared with mGlu2-A677S$^{4.40}$-eYFP + 5-HT$_{2A}$-mCherry, $F(2,28) = 0.76$, $p > 0.05$; mGlu2-eYFP + 5-HT$_{2A}$-mCherry compared with mGlu2-A681F$^{4.44}$-eYFP + 5-HT$_{2A}$-mCherry, $F(2,44) = 3.62$, $p < 0.05$; mGlu2-eYFP + 5-HT$_{2A}$-mCherry compared with mGlu2-A685G$^{4.48}$-eYFP + 5-HT$_{2A}$-mCherry: $F(2,36) = 3.70$, $p < 0.05$. *B,* FRET$_{max}$ obtained from individual FCM-based FRET saturation curves. Note that FRET$_{max}$ is significantly increased in mGlu2, mGlu2-A677S$^{4.40}$, mGlu2-A681F$^{4.44}$, and mGlu2-A685G$^{4.48}$ as compared with mGlu3. **, $p < 0.05$; **, $p < 0.01$; ***, $p < 0.001$; *n.s.*, not significant; Bonferroni's post hoc test of one-way ANOVA. *C,* fold change of FCM-based FRET signal for each combination of eYFP- or mCherry-tagged receptors (eYFP-tagged, donor; mCherry-tagged, acceptor). Data obtained in cells co-expressing either mGlu2, mGlu2-A677S$^{4.40}$/A681F$^{4.44}$, mGlu2-A677S$^{4.40}$/A685G$^{4.48}$, or mGlu2-A681F$^{4.44}$/A685G$^{4.48}$, all tagged with eYFP, and 5-HT$_{2A}$-mCherry can be fit preferably by a saturation curve, assessed by *F* test. Data obtained in cells co-expressing mGlu3-eYFP and 5-HT$_{2A}$-mCherry show linear correlations ($n = 8–23$). Note that mGlu2-A677S$^{4.40}$/A681F$^{4.44}$, mGlu2-A677S$^{4.40}$/A685G$^{4.48}$, mGlu2-A681F$^{4.44}$/A685G$^{4.48}$, or mGlu3 all decrease the FCM-based FRET signal as compared with mGlu2: mGlu2-eYFP + 5-HT$_{2A}$-mCherry compared with mGlu3-eYFP + 5-HT$_{2A}$-mCherry, $F(2,150) = 52.28$, $p < 0.001$; mGlu2-eYFP + 5-HT$_{2A}$-mCherry compared with mGlu2-A677S$^{4.40}$/A681F$^{4.44}$-eYFP + 5-HT$_{2A}$-mCherry, $F(2,106) = 14.96$, $p < 0.001$; mGlu2-eYFP + 5-HT$_{2A}$-mCherry compared with mGlu2-A677S$^{4.40}$/A685G$^{4.48}$-eYFP + 5-HT$_{2A}$-mCherry, $F(2,118) = 18.02$, $p < 0.001$; mGlu2-eYFP + 5-HT$_{2A}$-mCherry compared with mGlu2-A681F$^{4.44}$/A685G$^{4.48}$-eYFP + 5-HT$_{2A}$-mCherry, $F(2,121) = 13.97$, $p < 0.001$. *D,* FRET$_{max}$ obtained from individual FCM-based FRET saturation curves. Note that FRET$_{max}$ is significantly increased in mGlu2, but not in mGlu2-A677S$^{4.40}$/A681F$^{4.44}$, mGlu2-A677S$^{4.40}$/A685G$^{4.48}$, and mGlu2-A681F$^{4.44}$/Ala-685G$^{4.48}$, as compared with mGlu3. ***, $p < 0.001$; *n.s.*, not significant; Bonferroni's post hoc test of one-way ANOVA. *Error bars* represent S.E.

However, the high affinity component of the capacity of DOI to displace [^{3}H]ketanserin binding was decreased when mGlu2ΔTM4C and the 5-HT$_{2A}$ receptor were co-expressed, resulting in a monophasic displacement curve (Fig. 8*B* and Table 1).

Virus-mediated Overexpression of mGlu2 as a Receptor Heterocomplex with the 5-HT$_{2A}$ Receptor in Mouse Frontal Cortex Rescues Psychosis-like Behavior—We have previously demonstrated that the head-twitch murine behavioral response is reliably and robustly elicited by hallucinogens and is absent in 5-HT$_{2A}$-KO mice (28). We also showed that the head-twitch response induced by the hallucinogenic 5-HT$_{2A}$ agonist DOI was significantly decreased in mGlu2-KO mice (50). These results suggest that the mGlu2 receptor is necessary to induce a 5-HT$_{2A}$-dependent head-twitch response. However, whether heteromerization is required for this behavioral response remains unknown. To fully establish the role of the 5-HT$_{2A}$·mGlu2 receptor heterocomplex in the psychoactive-like effects induced by hallucinogenic drugs, we overexpressed either mGlu2 or mGlu2ΔTM4N in the frontal cortex of mGlu2-KO mice to examine whether this manipulation would regulate behavior. Mice received intra-frontal cortical injections of bicistronic herpes simplex 2 viral particles (HSV-2) expressing green fluorescent protein (GFP) and either mGlu2 or mGlu2ΔTM4N or GFP alone. First, we confirmed that the virus overexpresses mGlu2 or mGlu2ΔTM4N in mouse frontal cortex (Fig. 9, *A* and *B*). We next investigated the behavioral effects induced by hallucinogenic drugs in HSV-mGlu2 and HSV-mGlu2ΔTM4N mice and their HSV-GFP counterparts. Remarkably, we found that the head-twitch response induced by the hallucinogenic 5-HT$_{2A}$ agonist DOI was rescued in mGlu2-KO mice overexpressing mGlu2, but not mGlu2ΔTM4N, in the frontal cortex as compared with that

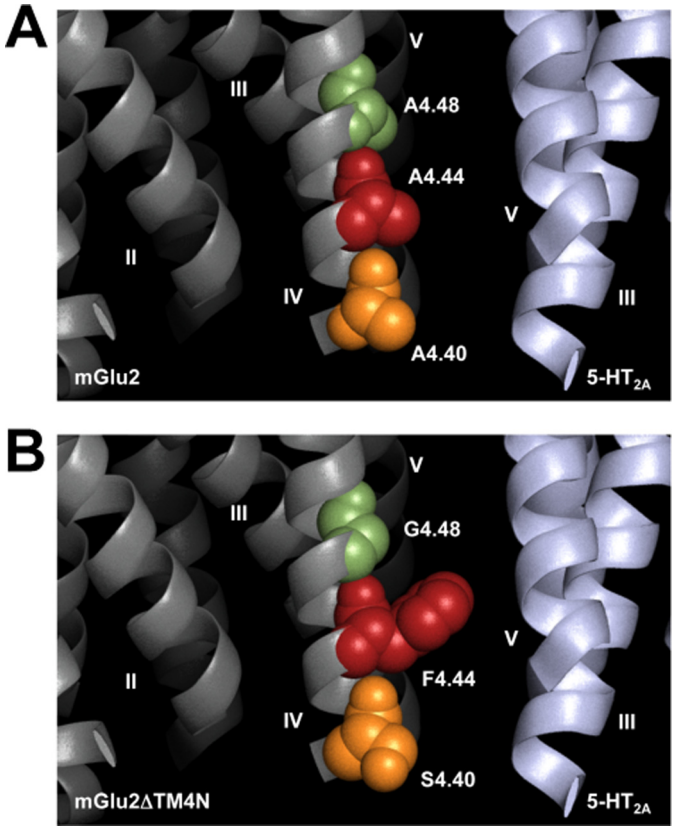

FIGURE 7. **Ala-677$^{4.40}$, Ala-681$^{4.44}$, and Ala-685$^{4.48}$ are critical for mGlu2 to form a receptor heteromer with 5-HT$_{2A}$.** *A, ribbon* backbone representation of the transmembrane helices of the 5-HT$_{2A}$·mGlu2 heteromer model. Residues Ala-677$^{4.40}$, Ala-681$^{4.44}$, and Ala-685$^{4.48}$ are shown as *spheres*. *B,* ribbon backbone representation of the transmembrane helices of the 5-HT$_{2A}$·mGlu2ΔTM4N heteromer model. Residues Ser-677$^{4.40}$, Phe-681$^{4.44}$, and Gly-685$^{4.48}$ are shown as *spheres*.

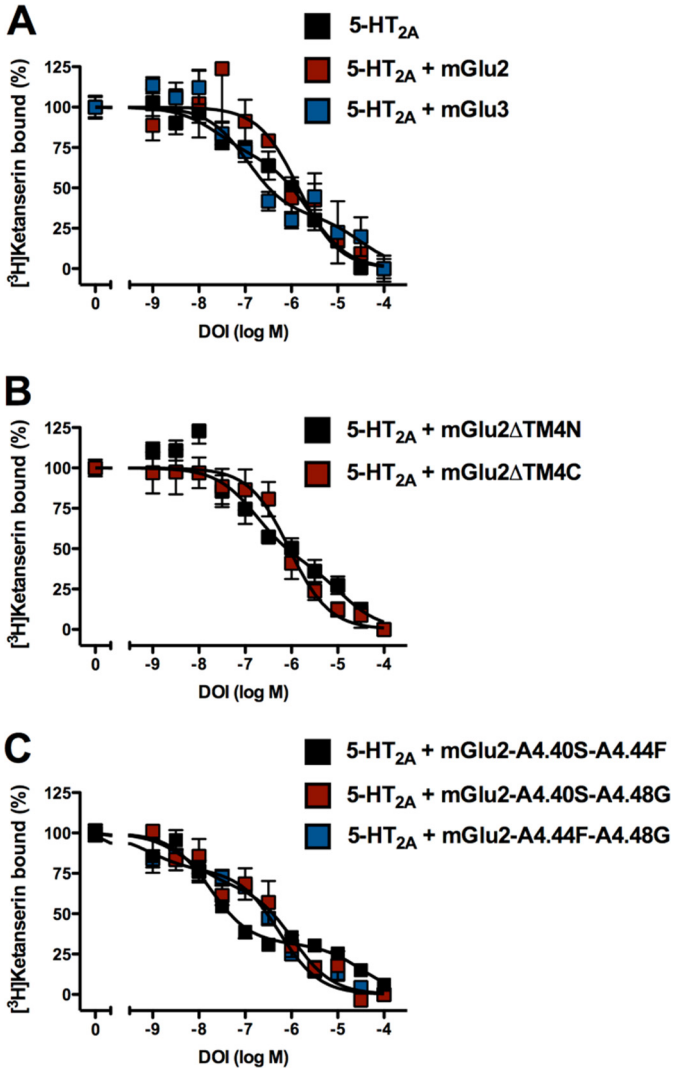

FIGURE 8. **Any two of the three residues located at the intracellular end of TM4 of mGlu2 affect allosteric cross-talk with the 5-HT$_{2A}$ receptor.** *A,* [^{3}H]ketanserin binding displacement curves by DOI in HEK293 cells co-expressing 5-HT$_{2A}$ and either mGlu2 or mGlu3 receptors. Note that the 5-HT$_{2A}$ affinity for DOI was decreased by mGlu2 and was unaffected by mGlu3 co-expression, assessed by *F* test ($n = 6$). *B,* [^{3}H]ketanserin binding displacement curves by DOI in HEK293 cells co-expressing 5-HT$_{2A}$ and either mGlu2ΔTM4N or mGlu2ΔTM4C chimera. Note that the 5-HT$_{2A}$ affinity for DOI was decreased by mGlu2ΔTM4C and was unaffected by mGlu2ΔTM4N co-expression, assessed by *F* test ($n = 6$). *C,* [^{3}H]ketanserin binding displacement curves by DOI in HEK293 cells co-expressing 5-HT$_{2A}$ and either mGlu2-A677S$^{4.40}$/A681F$^{4.44}$, mGlu2-A677S$^{4.40}$/A685G$^{4.48}$, or mGlu2-A681F$^{4.44}$/Ala-685G$^{4.48}$ chimera. Note that the 5-HT$_{2A}$ affinity for DOI was unaffected by mGlu2-A677S$^{4.40}$/A681F$^{4.44}$, mGlu2-A677S$^{4.40}$/A685G$^{4.48}$, or mGlu2-A681F$^{4.44}$/A685G$^{4.48}$ co-expression, assessed by *F* test ($n = 6$). *Error bars* represent S.E. See also Table 1 for statistical analysis.

seen in animals expressing GFP (Fig. 9*C*). Together, these findings indicate that the 5-HT$_{2A}$·mGlu2 receptor complex in the frontal cortex is critical for regulating psychosis-like states through a heteromeric interface that involves Ala-677$^{4.40}$, Ala-681$^{4.44}$, and Ala-685$^{4.48}$ at the cytoplasmic end of TM4 of the mGlu2 receptor.

Allosteric Cross-talk between mGlu2 and 5-HT$_{2A}$ Receptors in Post-mortem Human Brain of Schizophrenic Subjects—Although pharmacological models of neuropsychiatric disturbances have limitations (51), recent studies indicate that the clinical effects of hallucinogenic drugs, such as psilocybin, mescaline, and lysergic acid diethylamide, closely resemble a set of positive symptoms in schizophrenia (20, 52). We have previously shown that the 5-HT$_{2A}$ receptor is up-regulated and the mGlu2 receptor is down-regulated in the frontal cortex of post-mortem schizophrenic subjects (13, 53), a pattern of expression that could predispose to psychosis. The absence of the DOI-dependent head-twitch behavioral response in mice that do not express 5-HT$_{2A}$ and mGlu2 as a GPCR heteromer (see Fig. 9*C* above), together with the allosteric interaction between 5-HT$_{2A}$ and mGlu2 that we observed in tissue culture (see Fig. 8 above), led us to speculate that the functional cross-talk via the receptor heterocomplex might be dysregulated in the frontal cortex of schizophrenic subjects. We compared the effect of DOI on displacement of [^{3}H]LY341495 binding by LY379268 (selective mGlu2/3 antagonist and agonist, respectively) in frontal cortex membrane preparations of schizophrenic subjects and individually matched controls (see Table 2 for demographic information). As reported previously in mouse frontal cortex (13), competition binding experiments of [^{3}H]LY341495 were best described by a two-site model, and DOI (10 μM) decreased the high affinity component of LY379268 competition of [^{3}H]LY341495 binding in both schizophrenic subjects and controls (Fig. 10, *A–C*, and Table 3). The high affinity of LY379268 displacing [^{3}H]LY341495 binding was greater in the frontal cortex of schizophrenic subjects as compared with con-

trols (Fig. 10, *A–C*, and Table 3). No statistically significant differences were found between the low affinity of LY379268 displacing [^{3}H]LY341495 binding in schizophrenic subjects and individually matched controls (Table 3). Interestingly, we also found that the difference between the high affinities of LY379268 displacing [^{3}H]LY341495 binding in the presence and in the absence of DOI was significantly increased in the frontal cortex of schizophrenic subjects (Fig. 10*D*). No differences were observed between untreated and treated schizophrenic subjects (data not shown, see also Table 2 for demographic information). These findings suggest that the allosteric cross-talk between the components of the 5-HT$_{2A}$·mGlu2 receptor heterocomplex is dysregulated in the frontal cortex of schizophrenic subjects.

DISCUSSION

Although the interfaces of some family A GPCR homocomplexes have been studied extensively as regulators of ligand binding and receptor activation, the structural basis of GPCR heteromeric association is less well established. Similarly, the role of GPCR heteromers in whole animal models of pharmacology and behavior remains poorly understood. In this study, we provide evidence for the direct involvement of three residues located at the intracellular end of TM4 of the mGlu2 in being necessary for its heteromeric assembly with the 5-HT$_{2A}$ receptor. Our data reveal a critical role for Ala-677$^{4.40}$, Ala-681$^{4.44}$, and Ala-685$^{4.48}$ of mGlu2 in the expression of this receptor with the 5-HT$_{2A}$ receptor as a GPCR heterocomplex in tissue culture and mouse frontal cortex. We first show that substitution of these three residues with the ones located at equivalent positions in the TM4 of the closely related mGlu3 is sufficient to disrupt its heteromeric association with the 5-HT$_{2A}$ receptor in living cells. It is well known that expression of the mGlu2 receptor is necessary for the behavioral effects induced by hallucinogenic 5-HT$_{2A}$ agonists such as DOI and lysergic acid diethylamide in mouse models (16, 50). Although interesting, these data do not indicate directly whether the 5-HT$_{2A}$·mGlu2 heteromeric complex is necessary for the psychosis-like states induced by hallucinogenic drugs. We now demonstrate that virus-mediated overexpression of mGlu2 in frontal cortical neurons of mGlu2-KO mice rescues the head-twitch behavioral response induced by DOI, whereas overexpression of mGlu2 with Ala-677$^{4.40}$, Ala-681$^{4.44}$ and Ala-685$^{4.48}$ substituted by the corresponding residues of mGlu3 does not. Furthermore, our data reveal that Ala-677$^{4.40}$, Ala-681$^{4.44}$, and Ala-685$^{4.48}$ of mGlu2 are necessary for the allosteric binding interaction between the components of the 5-HT$_{2A}$·mGlu2 receptor heterocomplex, a functional cross-talk that we also found up-regulated in post-mortem frontal cortex of schizophrenic subjects as compared with that obtained in controls. These data provide the first evidence for the specific residues responsible for GPCR heteromeric complex formation, validate

TABLE 1

[^{3}H]Ketanserin binding displacement curves by DOI in HEK293 cells co-transfected with 5-HT$_{2A}$ and mGlu2/mGlu3 chimeras

DOI displacement of [^{3}H]ketanserin (4.0 nM; K_D = 7.1 nM) binding was performed in HEK293 cells co-transfected with 5-HT$_{2A}$ and mGlu2/mGlu3 chimeras. Competition curves were analyzed by nonlinear regression to derive dissociation constants for high ($K_{i\text{-high}}$) and low ($K_{i\text{-low}}$) affinity states of the receptor. % high refers to the percentage of high affinity binding sites as calculated from nonlinear fitting. Values are best fit ± S.E. of three experiments performed in duplicate. One- or two-site model as a better description of the data was determined by *F* test. Two-site model, $p < 0.05$. NA, two-site model not applicable, $p > 0.05$.

mGlu receptor	$K_{i\text{-high}}$ (log M)	$K_{i\text{-low}}$ (log M)	% High
Mock	−7.78 ± 0.4	−5.72 ± 0.2	31.2 ± 8.1
mGlu2	NA	−6.19 ± 0.2	NA
mGlu3	−7.25 ± 0.2	−3.83 ± 0.3	41 ± 8.5
mGlu2Δ TM4N	−7.21 ± 0.2	−4.92 ± 0.3	56.5 ± 6.4
mGlu2Δ TM4C	NA	−6.25 ± 0.1	NA
mGlu2-A4.40S-A4.44F	−7.97 ± 0.1	−5.01 ± 0.4	63.9 ± 11
mGlu2-A4.40S-A4.48G	−8.56 ± 0.4	−6.20 ± 0.2	33.6 ± 8.0
mGlu2-A4.44F-A4.48G	−8.68 ± 0.6	−6.56 ± 0.1	26.4 ± 7.4

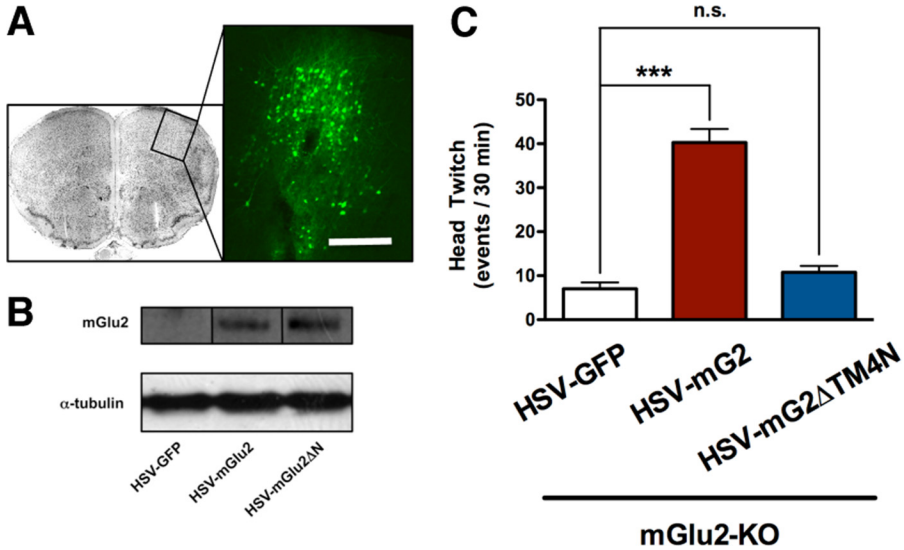

FIGURE 9. **Expression of mGlu2 as a receptor heterocomplex with 5-HT$_{2A}$ is necessary for psychosis-like behavior induced by hallucinogenic drugs.** *A,* representative image of HSV-mediated transgene expression in the frontal cortex. HSV-mGlu2, which also expresses GFP, was injected into frontal cortex, and GFP expression was revealed by immunocytochemistry. *Scale bar,* 200 μm. *B,* HSV-mediated transgene expression in mouse frontal cortex. HSV-GFP, HSV-mGlu2, and HSV-mGlu2ΔTM4N were injected into frontal cortex of mGlu2-KO mice, and anti-mGlu2 expression was measured by Western blotting. *C,* virus-mediated overexpression of mGlu2, but not mGlu2ΔTM4N, in the frontal cortex of mGlu2-KO mice significantly rescues the head-twitch response induced by the hallucinogenic 5-HT$_{2A}$ agonist DOI (0.5 mg/kg; $n = 4$ mice per group). ***, $p < 0.001$; *n.s*, not significant; Bonferroni's post hoc test of one-way ANOVA. *Error bars* represent S.E.

TABLE 2

Demographic characteristics and toxicological analysis of schizophrenic subjects (Sch) and their respective controls (C)

Antipsychotics were not detected in blood samples of antipsychotic-free (AP-free) schizophrenic subjects. Therapeutic levels of amisulpride (AMSP), clotiapine (CLT), clozapine (CLZ), haloperidol (HLP), olanzapine (OLZ), quetiapine (QTP), and sulpiride (SLP) were detected in blood samples of treated schizophrenia subjects. All schizophrenic subjects, except Sch 15, Sch 25, Sch 26, Sch 25, and Sch 27, committed suicide. Abbreviations used are as follow: AMP, amphetamine; ATR, atropine; BIP, biperiden; BNZG, benzoylecgonine; BZD, benzodiazepines or metabolites; CC, cocaine; CMI, clomipramine; CMZ, carbamazepine; HR, heroin; LDC, lidocaine; LVZ, levomepromazine; MET, metamizole; MPV, mepivacaine; PAR, paracetamol; PHBT, phenobarbital; PHEN, phenytoin; PROC, procainamide; and THC, tetrahydrocannabinol. Ethanol in blood is coded as ETH. Tissue pH values were within a relatively narrow range (control subjects, 6.41 ± 0.09; schizophrenic subjects, 6.51 ± 0.08). PMD is post-mortem delay; RIN is RNA integrity number. Group values are means ± S.E.

Case (C/Sch)	Gender (female (F)/male (M))	Age	PMD	Storage time	RIN	Antipsychotic treatment	Additional drugs
		years	*h*	*months*			
Sch1	M	21	24	175	8.5	AP-free	
C1	M	21	30	135	6.8		AMP, THC, ETH (0.24 g/liter)
Sch2	M	30	51	144	7.1	AP-free	
C2	M	29	18	32	5.3		
Sch3	M	29	6	79	8.4	AP-free	THC
C3	M	29	36	137	8.7		ETH (1.71 g/liter)
Sch4	M	31	14	78	7.7	AP-free	BZD
C4	M	32	28	78	8		AMP, ETH (0.68 g/liter)
Sch5	M	48	20	74	8.3	AP-free	
C5	M	47	18	94	7.8		BZD
Sch6	M	31	11	65	9.2	AP-free	
C6	M	31	13	51	8.2		ETH (0.96 g/liter)
Sch7	M	33	14	64	7.4	AP-free	BZD
C7	M	33	4	52	9.1		
Sch8	M	45	3	60	9.3	AP-free	BZD
C8	M	44	21	46	8.5		
Sch9	M	27	24	60	3.8	AP-free	
C9	M	28	30	132	8.3		
Sch10	F	37	58	44	7.4	AP-free	HR, BZD
C10	F	36	38	168	9		HR, BZD, CC
Sch11	M	46	22	35	8.2	AP-free	BIP
C11	M	46	24	23	8.5		
Sch12	F	37	23	9	8.3	AP-free	BZD
C12	F	38	22	6	7.6		
Sch13	M	48	11	9	8	AP-free	
C13	M	49	8	3	8.8		
Sch14	M	35	5	10	8.5	AP-free	
C14	M	38	33	165	7.6		ETH (1.62 g/liter)
Sch15	F	59	9	15	8.7	AP-free	
C15	F	58	20	136	7.2		
Sch16	M	45	18	19	5.4	AP-free	
C16	M	47	15	4	7.4		BZD, ETH (1.55 g/liter)
Sch17	M	34	15	21	8.9	AP-free	
C17	M	36	48	15	7.7		
Sch18	M	52	7	26	9.1	AP-free	BZD
C18	M	51	13	6	8.1		ETH (2,13 g/liter)
Sch19	M	44	7	84	8.2	CLT, LVZ	BZD, BIP
C19	M	44	23	4	7.9		
Sch20	M	30	18	81	4.9	OLZ	
C20	M	30	11	82	8		THC
Sch21	M	32	8	77	7.4	QTP	BZD, PAR
C21	M	32	20	135	6.7		ATR, LDC, ETH (2.37 g/liter)
Sch22	M	23	16	72	9.1	SLP	
C22	M	23	17	45	7.1		
Sch23	M	35	3	72	9.2	QTP	BZD
C23	M	36	23	4	8.2		
Sch24	F	30	28	66	2.9	HLP	BZD, PROC, MET, LDC, MPV
C24	F	29	31	171	9		
Sch25	M	35	11	24	8.6	CLZ	CMI, BZD, PAR
C25	M	36	18	94	9.2		BNZG, ETH (1.69 g/liter)
Sch26	F	60	23	14	5.5	AMSP, CLZ	BZD
C26	F	60	48	20	6.4		CMZ, PHEN, PHBT
Sch27	M	56	12	19	4	OLZ, CLT	
C27	M	54	16	10	8.2		ETH (0.58 g/liter)
Schizophrenia	22 M/5F	38 ± 2	17 ± 2	55 ± 8	7.5 ± 0.4		
Controls	22 M/5F	38 ± 2	23 ± 2	68 ± 11	7.9 ± 0.2		

the 5-HT$_{2A}$·mGlu2 receptor heterocomplex as necessary for the behavioral effects induced by lysergic acid diethylamide-like drugs in rodents, and reveal a potential role for this heteromeric receptor complex in the alterations in cognition and perception observed in schizophrenic patients.

The experimental identification of residues located at the interface of GPCR oligomeric structures has been the focus of significant attention. Recent years have seen great advances in determining crystal structures of family A GPCRs (54). Among these, crystal structures of GPCR subtypes, such as the photoactivated intermediate of rhodopsin (55), the β_2-adrenergic receptor bound to a partial inverse agonist (56), and the κ-opioid receptor bound to a selective antagonist (57), suggest that TM1 and the intracellular helix 8 following TM7 are located at the interface of the receptor homomer. However, in homomers of the CXCR4 receptor bound to an antagonist, the individual molecules interact only at the extracellular side of TM5 and TM6 (58). These differences suggest structural variability

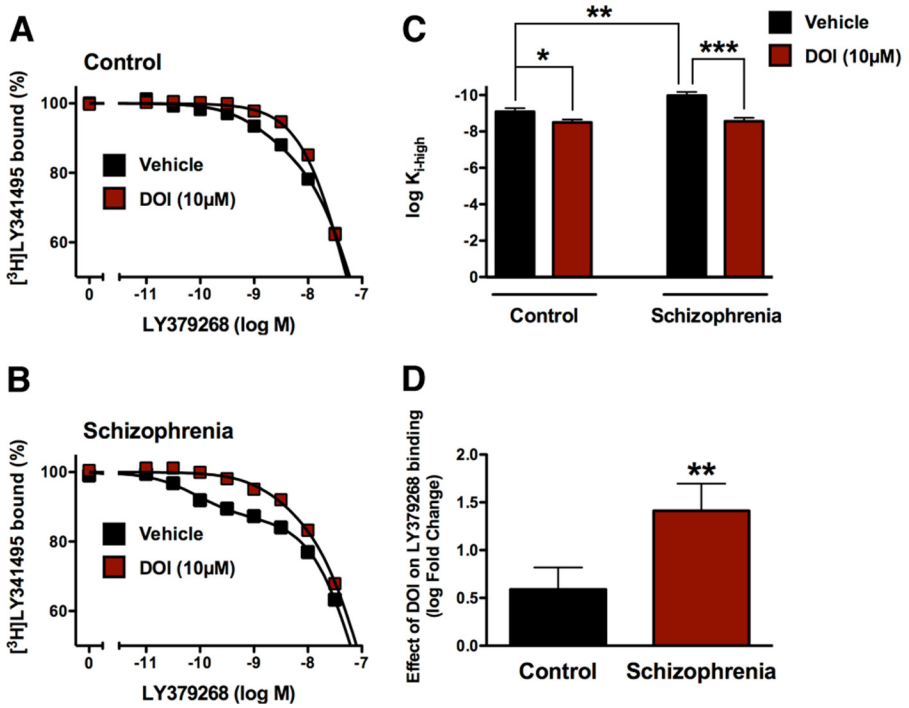

FIGURE 10. **Allosteric cross-talk between mGlu2 and 5-HT$_{2A}$ as a receptor heterocomplex is up-regulated in the post-mortem frontal cortex of schizophrenic subjects.** *A* and *B*, [^{3}H]LY341495 binding displacement curves by LY379268 in the frontal cortex membrane preparations of schizophrenic subjects and individually matched controls. Experiments were performed in the presence and in the absence of DOI (10 μM). Note that displacement curves of [^{3}H]LY341495 binding by LY379268 were statistically different in the presence of DOI, assessed by *F* test. *C*, affinity of LY379268 ($K_{i\text{-high}}$) displacing [^{3}H]LY341495 binding in post-mortem frontal cortex membrane preparations of schizophrenic subjects and individually matched controls. Note that, in the absence of DOI, the affinity of LY379268 displacing [^{3}H]LY341495 was significantly higher in schizophrenic subjects as compared with controls. Also note that DOI (10 μM) significantly decreased the affinity of LY379268 displacing [^{3}H]LY341495 binding in both schizophrenic subjects and controls. *, $p < 0.05$; **, $p < 0.01$; ***, $p < 0.001$; Student's *t* test. *D*, effect of DOI (10 μM) on the affinity of LY379268 displacing [^{3}H]LY341495 binding in post-mortem frontal cortex membrane preparations of schizophrenic subjects as compared with individually matched controls. Note that the effect of DOI is significantly higher in schizophrenic subjects. **, $p < 0.01$; Student's *t* test. *Error bars* represent S.E. See also Table 2 for demographic information, and Table 3 for statistical analysis.

TABLE 3

Effect of DOI on [^{3}H]LY341495 binding displacement curves by LY379268 in post-mortem frontal cortex of schizophrenic subjects ($n = 27$) and controls ($n = 27$)

LY379268 displacement of [^{3}H]LY341495 (5.0 nM; $K_D = 4.6$ nM) binding was performed in post-mortem frontal cortex of schizophrenic subjects and controls (see Table 2 for demographic information). Competition curves were analyzed by nonlinear regression to derive dissociation constants for high ($K_{i\text{-high}}$) and low ($K_{i\text{-low}}$) affinity states of the receptor. % high refers to the percentage of high affinity binding sites as calculated from nonlinear fitting. Values are best fit ± S.E. of experiments performed in triplicate. One- or two-site model as a better description of the data was determined by *F* test (two-site model, $p < 0.05$). Control-Vehicle, $F(2,348) = 76.21$, $p < 0.0001$; Control-DOI, $F(2,348) = 14.20$, $p < 0.0001$; Schizophrenia-Vehicle, $F(2,348) = 225.9$, $p < 0.0001$; Schizophrenia-DOI, $F(2,348) = 34.29$, $p < 0.0001$.

	Vehicle			DOI (10 μM)		
	$K_{i\text{-high}}$ (log M)	$K_{i\text{-low}}$ (log M)	% High	$K_{i\text{-high}}$ (log M)	$K_{i\text{-low}}$ (log M)	% High
Control	−9.08 ± 0.2	−7.40 ± 0.0	26.2 ± 4	−8.49 ± 0.2[a]	−6.74 ± 0.2	39.5 ± 6
Schizophrenia	−9.97 ± 0.2[b]	−7.38 ± 0.1	18.1 ± 2	−8.56 ± 0.2[c]	−7.29 ± 0.0	36.0 ± 5

[a] Effect of DOI on $K_{i\text{-high}}$, $p < 0.05$ as compared with vehicle (Student's *t* test).
[b] Differences between schizophrenia and controls, $p < 0.01$ as compared with control subjects (Student's *t* test).
[c] Effect of DOI on $K_{i\text{-high}}$, $p < 0.001$ as compared with vehicle (Student's *t* test).

among the interfaces of family A homomeric GPCRs. Another possible explanation for the differences observed between the TM domains located at the interface of family A GPCR homomeric complexes may be related to the effects of solubilization and crystallization on the oligomeric structure. The crystal structures of a photoactivated intermediate rhodopsin, the β_2-adrenergic receptor, and the κ-opioid receptor contain individual GPCR molecules that are packed in a parallel manner (55–57), which is the form that represents the physiologically relevant orientation. However, crystal structures of rhodopsin (24) and the A_{2A} adenosine receptor (59) revealed an anti-parallel association, suggesting that solubilization protocols may affect the location of the components of GPCR oligomers. Interestingly, experiments performed in native membranes by atomic force microscopy put forward that the interface between two rhodopsin molecules is likely to involve TM4 and TM5, whereas TM1 facilitates the formation of rhodopsin dimer rows (19). A similar conclusion has been reached *in vitro* in living cells with the dopamine D_2 homomeric receptor using a cysteine cross-linking assay (7, 43, 60). This assay represents a sensitive and specific method for detection of positions that are located in close molecular proximity to one another at the homomeric interface. Although interesting, it does not provide information as to whether the individual residues in close proximity are necessary to form the GPCR homomeric structure. Using the differences between mGlu2 and mGlu3 receptors in

the formation of a GPCR heteromeric complex with the 5-HT$_{2A}$ receptor, our findings demonstrate that three residues located at the intracellular end of TM4 are responsible for the location of the mGlu2 receptor in close molecular proximity to the 5-HT$_{2A}$ receptor at the plasma membrane in living cells. Our findings do not exclude a possible parallel interface along the entire TM4 of the mGlu2 receptor, but rather they provide compelling evidence of the individual residues that are necessary to form the 5-HT$_{2A}$·mGlu2 receptor heterocomplex. The importance of these three residues is further supported by the absence of allosteric cross-talk between 5-HT$_{2A}$ and mGlu2ΔTM4N, but not between 5-HT$_{2A}$ and mGlu2ΔTM4C, in cultured cells. Family A GPCRs such as α_{1b}-adrenergic and dopamine D$_2$ receptors have been shown to form higher order homo-oligomers (6, 7). However, convincing findings suggest that metabotropic glutamate receptors form strict dimers, and not higher order oligomers, at the cell surface (61). Further investigation will be needed to assess the potential expression of 5-HT$_{2A}$ and mGlu2 as a higher order oligomer in living cells.

One of the main concerns regarding the existence of GPCR heterocomplexes is the specificity and sensitivity of the biochemical studies *in vitro* in tissue culture, as well as the evidence for molecular proximity *in vivo* in native tissue. In this study, we show that 5-HT$_{2A}$ and mGlu2 receptors form a stable protein complex, as it resists the protocol of plasma membrane preparation and solubilization followed by co-immunoprecipitation experiments in HEK293 cells (see Fig. 2*A*) and in native tissue (13, 16). However, a potential caveat of studies involving co-immunoprecipitation of epitope-tagged receptors is the hydrophobicity of the TM domains of GPCRs, which raises the concerns of nonspecific aggregation following detergent extraction of proteins from plasma membrane preparations (48). We observed the absence of co-immunoprecipitation in cells expressing only one of the tagged receptors and combined prior to the immunoprecipitation step. Together with the absence of co-immunoprecipitation of HA-mGlu3 when co-expressed with c-Myc-5-HT$_{2A}$, this eliminates nonspecific aggregation as a potential explanation of co-immunoprecipitation, and it supports the specificity of the co-immunoprecipitation assay in plasma membrane preparations. The conclusion that 5-HT$_{2A}$ and mGlu2 receptors are located in close molecular proximity in living cells is also reached based upon our results showing FRET signal between mGlu2-eYFP and 5-HT$_{2A}$-mCherry but not between mGlu3-eYFP and 5-HT$_{2A}$-mCherry. Similar findings were obtained when the donor and acceptor fluorophores were swapped in FCM-based FRET and FRET microscopy assays. Importantly, wild type and chimeric receptors show comparable levels of expression as determined by radioligand binding, flow cytometry, and immunocytochemistry. Together, these findings suggest that random collision is not the mechanism underlying the FCM-based FRET signal obtained in tissue culture.

A notable finding of this study is that 5-HT$_{2A}$ and mGlu2 receptors form a GPCR heteromeric complex with specific functional outcomes in native tissue. We previously found an allosteric cross-talk between the components of the 5-HT$_{2A}$·mGlu2 receptor heterocomplex in mouse frontal cortex plasma membrane preparations (13). Our findings now demonstrate that Ala-677$^{4.40}$, Ala-681$^{4.44}$, and Ala-685$^{4.48}$ of mGlu2 are necessary for this pharmacological property of the 5-HT$_{2A}$·mGlu2 receptor heterocomplex to occur, with validation of the allosteric cross-talk in post-mortem human frontal cortex. These findings, together with the alterations in the allosteric cross-talk between 5-HT$_{2A}$ and mGlu2 as a receptor heterocomplex that we observed in post-mortem frontal cortex of schizophrenic subjects, point toward a possible role for this GPCR heterocomplex in the etiology of schizophrenia and psychosis.

Although further investigation is needed to characterize quantitatively their ultrastructural co-localization in human and mouse CNS, here we provide evidence of subcellular co-immunolocalization and close physical proximity of 5-HT$_{2A}$ and mGlu2 receptors at cortical synaptic junctions at the electron microscopy level. Previous studies convincingly demonstrate that the cellular, electrophysiological and behavioral responses induced by hallucinogenic drugs in mouse models are intrinsic to 5-HT$_{2A}$ receptor-expressing cortical pyramidal neurons (28, 62, 63). Because HSV-mediated overexpression of mGlu2, but not mGlu2ΔTM4N, in frontal cortical neurons of mGlu2-KO mice rescues the head-twitch behavior induced by the hallucinogenic 5-HT$_{2A}$ receptor agonist DOI, together, these findings provide the first evidence that cortical 5-HT$_{2A}$·mGlu2 receptor heterocomplex is necessary for at least some of the psychoactive effects of hallucinogenic drugs.

In summary, we show that expression of 5-HT$_{2A}$ and mGlu2 as a GPCR heteromer in the frontal cortex is important for regulating psychosis-like behavior in mice and is potentially involved in the altered cortical processes of schizophrenia. These findings extend our understanding of the molecular basis of psychosis and may provide a route to the development of new and more effective drugs for the treatment of schizophrenia and other psychotic disorders.

Acknowledgments—We thank Drs. Lakshmi Devi, Miguel Fribourg, and Iban Ubarretxena (Mount Sinai School of Medicine), Paula Bos (Memorial Sloan-Kettering Cancer Center), and Diomedes Logothetis (Virginia Commonwealth University School of Medicine) for their critical review of the manuscript; Dr. Jordi Ochando for help in FCM experiments; Dr. Jay Gingrich for the gift of 5HT2A-KO mice; Vinayak Rayannavar and John Pediani for assistance with biochemical, behavioral, and FRET microscopy assays; and the staff members of the Basque Institute of Legal Medicine for their cooperation in the study.

REFERENCES

1. Pierce, K. L., Premont, R. T., and Lefkowitz, R. J. (2002) Seven-transmembrane receptors. *Nat. Rev. Mol. Cell Biol.* **3,** 639–650
2. Perez, D. M. (2003) The evolutionarily triumphant G-protein-coupled receptor. *Mol. Pharmacol.* **63,** 1202–1205
3. Rosenbaum, D. M., Rasmussen, S. G., and Kobilka, B. K. (2009) The structure and function of G-protein-coupled receptors. *Nature* **459,** 356–363
4. Whorton, M. R., Bokoch, M. P., Rasmussen, S. G., Huang, B., Zare, R. N., Kobilka, B., and Sunahara, R. K. (2007) A monomeric G protein-coupled receptor isolated in a high-density lipoprotein particle efficiently activates its G protein. *Proc. Natl. Acad. Sci. U.S.A.* **104,** 7682–7687
5. Whorton, M. R., Jastrzebska, B., Park, P. S., Fotiadis, D., Engel, A., Palczewski, K., and Sunahara, R. K. (2008) Efficient coupling of transducin to monomeric rhodopsin in a phospholipid bilayer. *J. Biol. Chem.* **283,** 4387–4394

6. Lopez-Gimenez, J. F., Canals, M., Pediani, J. D., and Milligan, G. (2007) The α1b-adrenoceptor exists as a higher order oligomer. Effective oligomerization is required for receptor maturation, surface delivery, and function. *Mol. Pharmacol.* **71,** 1015–1029
7. Guo, W., Urizar, E., Kralikova, M., Mobarec, J. C., Shi, L., Filizola, M., and Javitch, J. A. (2008) Dopamine D_2 receptors form higher order oligomers at physiological expression levels. *EMBO J.* **27,** 2293–2304
8. Fung, J. J., Deupi, X., Pardo, L., Yao, X. J., Velez-Ruiz, G. A., Devree, B. T., Sunahara, R. K., and Kobilka, B. K. (2009) Ligand-regulated oligomerization of β_2-adrenoceptors in a model lipid bilayer. *EMBO J.* **28,** 3315–3328
9. Hern, J. A., Baig, A. H., Mashanov, G. I., Birdsall, B., Corrie, J. E., Lazareno, S., Molloy, J. E., and Birdsall, N. J. (2010) Formation and dissociation of M1 muscarinic receptor dimers seen by total internal reflection fluorescence imaging of single molecules. *Proc. Natl. Acad. Sci. U.S.A.* **107,** 2693–2698
10. Milligan, G. (2009) G protein-coupled receptor hetero-dimerization. Contribution to pharmacology and function. *Br. J. Pharmacol.* **158,** 5–14
11. Prezeau, L., Rives, M. L., Comps-Agrar, L., Maurel, D., Kniazeff, J., and Pin, J. P. (2010) Functional cross-talk between GPCRs: with or without oligomerization. *Curr. Opin. Pharmacol.* **10,** 6–13
12. Carriba, P., Navarro, G., Ciruela, F., Ferré, S., Casadó, V., Agnati, L., Cortés, A., Mallol, J., Fuxe, K., Canela, E. I., Lluís, C., and Franco, R. (2008) Detection of heteromerization of more than two proteins by sequential BRET-FRET. *Nat. Methods* **5,** 727–733
13. González-Maeso, J., Ang, R. L., Yuen, T., Chan, P., Weisstaub, N. V., López-Giménez, J. F., Zhou, M., Okawa, Y., Callado, L. F., Milligan, G., Gingrich, J. A., Filizola, M., Meana, J. J., and Sealfon, S. C. (2008) Identification of a serotonin/glutamate receptor complex implicated in psychosis. *Nature* **452,** 93–97
14. Vilardaga, J. P., Nikolaev, V. O., Lorenz, K., Ferrandon, S., Zhuang, Z., and Lohse, M. J. (2008) Conformational cross-talk between α2A-adrenergic and μ-opioid receptors controls cell signaling. *Nat. Chem. Biol.* **4,** 126–131
15. Urizar, E., Yano, H., Kolster, R., Galés, C., Lambert, N., and Javitch, J. A. (2011) CODA-RET reveals functional selectivity as a result of GPCR heteromerization. *Nat. Chem. Biol.* **7,** 624–630
16. Fribourg, M., Moreno, J. L., Holloway, T., Provasi, D., Baki, L., Mahajan, R., Park, G., Adney, S. K., Hatcher, C., Eltit, J. M., Ruta, J. D., Albizu, L., Li, Z., Umali, A., Shim, J., Fabiato, A., MacKerell, A. D., Jr., Brezina, V., Sealfon, S. C., Filizola, M., González-Maeso, J., and Logothetis, D. E. (2011) Decoding the signaling of a GPCR heteromeric complex reveals a unifying mechanism of action of antipsychotic drugs. *Cell* **147,** 1011–1023
17. Tsuji, Y., Shimada, Y., Takeshita, T., Kajimura, N., Nomura, S., Sekiyama, N., Otomo, J., Usukura, J., Nakanishi, S., and Jingami, H. (2000) Cryptic dimer interface and domain organization of the extracellular region of metabotropic glutamate receptor subtype 1. *J. Biol. Chem.* **275,** 28144–28151
18. Margeta-Mitrovic, M., Jan, Y. N., and Jan, L. Y. (2000) A trafficking checkpoint controls $GABA_B$ receptor heterodimerization. *Neuron* **27,** 97–106
19. Liang, Y., Fotiadis, D., Filipek, S., Saperstein, D. A., Palczewski, K., and Engel, A. (2003) Organization of the G protein-coupled receptors rhodopsin and opsin in native membranes. *J. Biol. Chem.* **278,** 21655–21662
20. González-Maeso, J., and Sealfon, S. C. (2009) Psychedelics and schizophrenia. *Trends Neurosci.* **32,** 225–232
21. Aghajanian, G. K. (2009) Modeling "psychosis" *in vitro* by inducing disordered neuronal network activity in cortical brain slices. *Psychopharmacology* **206,** 575–585
22. Gordon, G. W., Berry, G., Liang, X. H., Levine, B., and Herman, B. (1998) Quantitative fluorescence resonance energy transfer measurements using fluorescence microscopy. *Biophys. J.* **74,** 2702–2713
23. Rasmussen, S. G., Choi, H. J., Rosenbaum, D. M., Kobilka, T. S., Thian, F. S., Edwards, P. C., Burghammer, M., Ratnala, V. R., Sanishvili, R., Fischetti, R. F., Schertler, G. F., Weis, W. I., and Kobilka, B. K. (2007) Crystal structure of the human β2 adrenergic G-protein-coupled receptor. *Nature* **450,** 383–387
24. Palczewski, K., Kumasaka, T., Hori, T., Behnke, C. A., Motoshima, H., Fox, B. A., Le Trong, I., Teller, D. C., Okada, T., Stenkamp, R. E., Yamamoto, M., and Miyano, M. (2000) Crystal structure of rhodopsin. A G protein-coupled receptor. *Science* **289,** 739–745
25. Kiefer, F., Arnold, K., Künzli, M., Bordoli, L., and Schwede, T. (2009) The SWISS-MODEL repository and associated resources. *Nucleic Acids Res.* **37,** D387–D392
26. Binet, V., Duthey, B., Lecaillon, J., Vol, C., Quoyer, J., Labesse, G., Pin, J. P., and Prézeau, L. (2007) Common structural requirements for heptahelical domain function in class A and class C G protein-coupled receptors. *J. Biol. Chem.* **282,** 12154–12163
27. DeLano, W. L. (2002) *The PyMOL Molecular Graphics System,* DeLano Scientific LLc, San Carlos, CA
28. González-Maeso, J., Weisstaub, N. V., Zhou, M., Chan, P., Ivic, L., Ang, R., Lira, A., Bradley-Moore, M., Ge, Y., Zhou, Q., Sealfon, S. C., and Gingrich, J. A. (2007) Hallucinogens recruit specific cortical 5-HT(2A) receptor-mediated signaling pathways to affect behavior. *Neuron* **53,** 439–452
29. Yokoi, M., Kobayashi, K., Manabe, T., Takahashi, T., Sakaguchi, I., Katsuura, G., Shigemoto, R., Ohishi, H., Nomura, S., Nakamura, K., Nakao, K., Katsuki, M., and Nakanishi, S. (1996) Impairment of hippocampal mossy fiber LTD in mice lacking mGluR2. *Science* **273,** 645–647
30. American Psychiatric Association (eds) (1994) *Diagnostic and Statistical Manual of Mental Disorders*, DSM-IV, 4th Ed., Washington, D. C.
31. García-Sevilla, J. A., Alvaro-Bartolomé, M., Díez-Alarcia, R., Ramos-Miguel, A., Puigdemont, D., Pérez, V., Alvarez, E., and Meana, J. J. (2010) Reduced platelet G protein-coupled receptor kinase 2 in major depressive disorder. Antidepressant treatment-induced up-regulation of GRK2 protein discriminates between responder and nonresponder patients. *Eur. Neuropsychopharmacol.* **20,** 721–730
32. Mortillo, S., Elste, A., Ge, Y., Patil, S. B., Hsiao, K., Huntley, G. W., Davis, R. L., and Benson, D. L. (2012) Compensatory redistribution of neuroligins and N-cadherin following deletion of synaptic β1-integrin. *J. Comp. Neurol.* **520,** 2041–2052
33. Kurita, M., Holloway, T., García-Bea, A., Kozlenkov, A., Friedman, A. K., Moreno, J. L., Heshmati, M., Golden, S. A., Kennedy, P. J., Takahashi, N., Dietz, D. M., Mocci, G., Gabilondo, A. M., Hanks, J., Umali, A., Callado, L. F., Gallitano, A. L., Neve, R. L., Shen, L., Buxbaum, J. D., Han, M. H., Nestler, E. J., Meana, J. J., Russo, S. J., and González-Maeso, J. (2012) HDAC2 regulates atypical antipsychotic responses through the modulation of mGlu2 promoter activity. *Nat. Neurosci.* **15,** 1245–1254
34. Hof, P. R., Young, W. G., Bloom, F. E., Belichenko, P. V., and Celio, M. R. (2000) *Comparative Cytoarchitectonic Atlas of the C57BL/6 and 129/Sv Mouse Brains*, pp. 129–239, Elsevier Science BV, Amsterdam, The Netherlands
35. González-Maeso, J., Yuen, T., Ebersole, B. J., Wurmbach, E., Lira, A., Zhou, M., Weisstaub, N., Hen, R., Gingrich, J. A., and Sealfon, S. C. (2003) Transcriptome fingerprints distinguish hallucinogenic and nonhallucinogenic 5-hydroxytryptamine 2A receptor agonist effects in mouse somatosensory cortex. *J. Neurosci.* **23,** 8836–8843
36. Vollenweider, F. X., Leenders, K. L., Scharfetter, C., Maguire, P., Stadelmann, O., and Angst, J. (1997) Positron emission tomography and fluorodeoxyglucose studies of metabolic hyperfrontality and psychopathology in the psilocybin model of psychosis. *Neuropsychopharmacology* **16,** 357–372
37. Carhart-Harris, R. L., Erritzoe, D., Williams, T., Stone, J. M., Reed, L. J., Colasanti, A., Tyacke, R. J., Leech, R., Malizia, A. L., Murphy, K., Hobden, P., Evans, J., Feilding, A., Wise, R. G., and Nutt, D. J. (2012) Neural correlates of the psychedelic state as determined by fMRI studies with psilocybin. *Proc. Natl. Acad. Sci. U.S.A.* **109,** 2138–2143
38. Marek, G. J., Wright, R. A., Schoepp, D. D., Monn, J. A., and Aghajanian, G. K. (2000) Physiological antagonism between 5-hydroxytryptamine(2A) and group II metabotropic glutamate receptors in prefrontal cortex. *J. Pharmacol. Exp. Ther.* **292,** 76–87
39. Wright, R. A., Johnson, B. G., Zhang, C., Salhoff, C., Kingston, A. E., Calligaro, D. O., Monn, J. A., Schoepp, D. D., and Marek, G. J. (2012) CNS distribution of metabotropic glutamate 2 and 3 receptors. Transgenic mice and [^{3}H]LY459477 autoradiography. *Neuropharmacology,*
40. Pin, J. P., Neubig, R., Bouvier, M., Devi, L., Filizola, M., Javitch, J. A., Lohse, M. J., Milligan, G., Palczewski, K., Parmentier, M., and Spedding, M. (2007) International Union of Basic and Clinical Pharmacology. LXVII. Recommendations for the recognition and nomenclature of G protein-coupled receptor heteromultimers. *Pharmacol. Rev.* **59,** 5–13

41. Ohishi, H., Neki, A., and Mizuno, N. (1998) Distribution of a metabotropic glutamate receptor, mGluR2, in the central nervous system of the rat and mouse. An immunohistochemical study with a monoclonal antibody. *Neurosci. Res.* **30,** 65–82
42. Jakab, R. L., and Goldman-Rakic, P. S. (1998) 5-Hydroxytryptamine 2A serotonin receptors in the primate cerebral cortex. Possible site of action of hallucinogenic and antipsychotic drugs in pyramidal cell apical dendrites. *Proc. Natl. Acad. Sci. U.S.A.* **95,** 735–740
43. Guo, W., Shi, L., Filizola, M., Weinstein, H., and Javitch, J. A. (2005) Crosstalk in G protein-coupled receptors. Changes at the transmembrane homodimer interface determine activation. *Proc. Natl. Acad. Sci. U.S.A.* **102,** 17495–17500
44. Ballesteros, J. A., and Weinstein, H. (1995) Integrated methods for the construction of three-dimensional models and computational probing of structure-function relations in G protein-coupled receptors. *Methods Neurosci.* **25,** 366–428
45. Magalhaes, A. C., Holmes, K. D., Dale, L. B., Comps-Agrar, L., Lee, D., Yadav, P. N., Drysdale, L., Poulter, M. O., Roth, B. L., Pin, J. P., Anisman, H., and Ferguson, S. S. (2010) CRF receptor 1 regulates anxiety behavior via sensitization of 5-HT2 receptor signaling. *Nat. Neurosci.* **13,** 622–629
46. Banning, C., Votteler, J., Hoffmann, D., Koppensteiner, H., Warmer, M., Reimer, R., Kirchhoff, F., Schubert, U., Hauber, J., and Schindler, M. (2010) A flow cytometry-based FRET assay to identify and analyse protein-protein interactions in living cells. *PloS ONE* **5,** e9344
47. Filizola, M., and Weinstein, H. (2005) The structure and dynamics of GPCR oligomers. A new focus in models of cell-signaling mechanisms and drug design. *Curr. Opin. Drug Discov. Devel.* **8,** 577–584
48. Milligan, G., and Bouvier, M. (2005) Methods to monitor the quaternary structure of G protein-coupled receptors. *FEBS J.* **272,** 2914–2925
49. Rovira, X., Pin, J. P., and Giraldo, J. (2010) The asymmetric/symmetric activation of GPCR dimers as a possible mechanistic rationale for multiple signaling pathways. *Trends Pharmacol. Sci.* **31,** 15–21
50. Moreno, J. L., Holloway, T., Albizu, L., Sealfon, S. C., and González-Maeso, J. (2011) Metabotropic glutamate mGlu2 receptor is necessary for the pharmacological and behavioral effects induced by hallucinogenic 5-HT2A receptor agonists. *Neurosci. Lett.* **493,** 76–79
51. Nestler, E. J., and Hyman, S. E. (2010) Animal models of neuropsychiatric disorders. *Nat. Neurosci.* **13,** 1161–1169
52. Vollenweider, F. X., Vollenweider-Scherpenhuyzen, M. F., Bäbler, A., Vogel, H., and Hell, D. (1998) Psilocybin induces schizophrenia-like psychosis in humans via a serotonin-2 agonist action. *Neuroreport* **9,** 3897–3902
53. Muguruza, C., Moreno, J. L., Umali, A., Callado, L. F., Meana, J. J., and Gonzalez-Maeso, J. (2012) Dysregulated 5-HT2A receptor binding in post-mortem frontal cortex of schizophrenic subjects. *Eur. Neuropsychopharmacol.,* in press
54. Shoichet, B. K., and Kobilka, B. K. (2012) Structure-based drug screening for G-protein-coupled receptors. *Trends Pharmacol. Sci.* **33,** 268–272
55. Salom, D., Lodowski, D. T., Stenkamp, R. E., Le Trong, I., Golczak, M., Jastrzebska, B., Harris, T., Ballesteros, J. A., and Palczewski, K. (2006) Crystal structure of a photoactivated deprotonated intermediate of rhodopsin. *Proc. Natl. Acad. Sci. U.S.A.* **103,** 16123–16128
56. Cherezov, V., Rosenbaum, D. M., Hanson, M. A., Rasmussen, S. G., Thian, F. S., Kobilka, T. S., Choi, H. J., Kuhn, P., Weis, W. I., Kobilka, B. K., and Stevens, R. C. (2007) High-resolution crystal structure of an engineered human β2-adrenergic G protein-coupled receptor. *Science* **318,** 1258–1265
57. Wu, H., Wacker, D., Mileni, M., Katritch, V., Han, G. W., Vardy, E., Liu, W., Thompson, A. A., Huang, X. P., Carroll, F. I., Mascarella, S. W., Westkaemper, R. B., Mosier, P. D., Roth, B. L., Cherezov, V., and Stevens, R. C. (2012) Structure of the human κ-opioid receptor in complex with JDTic. *Nature* **485,** 327–332
58. Wu, B., Chien, E. Y., Mol, C. D., Fenalti, G., Liu, W., Katritch, V., Abagyan, R., Brooun, A., Wells, P., Bi, F. C., Hamel, D. J., Kuhn, P., Handel, T. M., Cherezov, V., and Stevens, R. C. (2010) Structures of the CXCR4 chemokine GPCR with small-molecule and cyclic peptide antagonists. *Science* **330,** 1066–1071
59. Jaakola, V. P., Griffith, M. T., Hanson, M. A., Cherezov, V., Chien, E. Y., Lane, J. R., Ijzerman, A. P., and Stevens, R. C. (2008) The 2.6 angstrom crystal structure of a human A2A adenosine receptor bound to an antagonist. *Science* **322,** 1211–1217
60. Fonseca, J. M., and Lambert, N. A. (2009) Instability of a class a G protein-coupled receptor oligomer interface. *Mol. Pharmacol.* **75,** 1296–1299
61. Maurel, D., Comps-Agrar, L., Brock, C., Rives, M. L., Bourrier, E., Ayoub, M. A., Bazin, H., Tinel, N., Durroux, T., Prézeau, L., Trinquet, E., and Pin, J. P. (2008) Cell-surface protein-protein interaction analysis with time-resolved FRET and snap-tag technologies. Application to GPCR oligomerization. *Nat. Methods* **5,** 561–567
62. Béïque, J. C., Imad, M., Mladenovic, L., Gingrich, J. A., and Andrade, R. (2007) Mechanism of the 5-hydroxytryptamine 2A receptor-mediated facilitation of synaptic activity in prefrontal cortex. *Proc. Natl. Acad. Sci. U.S.A.* **104,** 9870–9875
63. Celada, P., Puig, M. V., Díaz-Mataix, L., and Artigas, F. (2008) The hallucinogen DOI reduces low-frequency oscillations in rat prefrontal cortex. Reversal by antipsychotic drugs. *Biol. Psychiatry* **64,** 392–400